



جامعة خليفة  
Khalifa University

# **Satellite Solar Array Configuration for Maximum Power Output for LEO**

Fatima Mohammed Alketbi

MSc in Mechanical Engineering

May 2020

A thesis submitted to Khalifa University of Science and Technology in accordance with the requirements of the degree of M.Sc. in Mechanical Engineering in the Department of Mechanical Engineering.



جامعة خليفة  
Khalifa University

# Satellite Solar Array Configuration for Maximum Power Output for LEO

by

Fatima Mohammed Alketbi

A thesis submitted in partial fulfillment of the  
requirements for the degree of

**MSc in Mechanical Engineering**

at

**Khalifa University**

## **Thesis Committee**

Dr. Firas Jarrar,

*Khalifa University*

Dr. Prashanth Marpu,

*Khalifa University*

Dr. MD Didarul Islam,

*Khalifa University*

Dr. Yap Yit Fatt,

*Khalifa University*

May 2020

# Abstract

Fatima Alketbi, “**Satellite Solar Array Configuration for Maximum Power Output For LEO**”, M.Sc. Thesis, MSc in Mechanical Engineering, Department of Mechanical Engineering, Khalifa University of Science and Technology, United Arab Emirates, May 2020.

CubeSats are widely used in scientific missions because they have low development costs and they are easily manufactured compared to the traditional satellites. The power system of a CubeSat depends on solar power which is limited due the area limitation and eclipse environment. The power generation could be enhanced by adding deployable solar panels. An available MATLAB algorithm for estimating the power generation throughout the orbit was both investigated and verified in this thesis. A verification of the validity of the code was conducted by using two different tools which are the Satellite Tool Kit (STK) and CubeSat Toolbox on MATLAB. The power generation code was used to analyze the power generation throughout the orbit for two 3U CubeSat models with different solar panels configurations in LEO. Model1 is a vertical 3U CubeSat with respect to the Z direction and it includes five different solar panels configurations whereas Model2 has horizontal orientation with three different solar panels configurations. The analyses showed that, the power could be enhanced by deploying the body-mounted solar panels or by adding deployable solar panels. The results show that 90-degree deployment angle is more efficient in Model1. However, the 45-degree deployment angle is more efficient in Model2. In addition, estimations of self-shadowing effect caused by the deployable solar panels on the body-mounted solar panels and on the total power generation was carried by using the CubeSat Toolbox on MATLAB. The self-shadowing effect could reduce the power generation by almost 10% which is a critical percentage for power budget calculations.

**Indexing Terms:** CubeSat, Solar panel, Solar panel configuration, Deployable solar panels, Power generation, self-shadowing.

# Acknowledgement

I would like to express my gratitude to my advisor, Dr. Firas Jarrar for his constant support, guidance throughout this research, and patience. Thank you for your kindness and for all you have taught me.

I would like to thank my co-advisor, Dr. Prashanth Marpu for allowing me to use the facilities available in the YahSat Space Lab where I had the full access to use the software.

I would also like to thank my colleagues from YahSat Space Lab, Rzan Al-Haddad and Nouf Alzaabi for their help with editing the code and explaining some parts of it. Thank you for your time and efforts.

Finally, I would like to thank my family, my husband, and my friends for their support and great love all the time. I am very grateful for you all and wouldn't have done it without you.

# Declaration and Copyright

## Declaration

I declare that the work in this thesis was carried out in accordance with the regulations of Khalifa University of Science and Technology. The work is entirely my own except where indicated by special reference in the text. Any views expressed in the thesis are those of the author and in no way represent those of Khalifa University of Science and Technology. No part of the thesis has been presented to any other university for any degree.

Author Name: Fatima Mohammed Alketbi

Author Signature:



Date: 29 May 2020

## Copyright ©

No part of this thesis may be reproduced, stored in a retrieval system, or transmitted, in any form or by any means, electronic, mechanical, photocopying, recording, scanning or otherwise, without prior written permission of the author. The thesis may be made available for consultation in Khalifa University of Science and Technology Library and for inter-library lending for use in another library and may be copied in full or in part for any bona fide library or research worker, on the understanding that users are made aware of their obligations under copyright, i.e. that no quotation and no information derived from it may be published without the author's prior consent.

# Contents

Abstract.....	I
Acknowledgement .....	II
Declaration and Copyright.....	III
Contents .....	IV
List of Figures.....	VI
List of Tables .....	IX
List of Abbreviations .....	X
List of Symbols.....	XI
<b>1</b> Introduction.....	1
1.1 Background .....	1
CubeSat.....	1
Power generation .....	2
Orbit definition.....	4
1.2 Problem Statement and Research Objectives.....	6
2 Literature Review.....	8
3 Methodology.....	12
3.1 Orbit and satellite definition.....	13
3.2 Orbit simulation.....	13
3.3 Power generation calculations.....	14
4 Verification of the code .....	21
4.1 STK results.....	21
CubeSat model.....	21
Analysis parameters .....	22
Analysis results .....	22
4.2 CubeSat Toolbox results .....	25

CubeSat model .....	25
Analysis parameters .....	25
Analysis results .....	26
5 Power Generation for different 3U CubeSat models .....	28
5.1 Model1 .....	28
5.2 Model2 .....	29
5.3 Analysis results .....	29
6 Self-shadowing .....	37
6.1 Simulation parameters.....	37
6.2 Self-shadowing analysis results .....	38
BM-DP-V-90 .....	39
BM-DP-V-45 .....	41
BM-DP-H-90 .....	43
BM-DP-H-45 .....	44
6.3 Self-shadowing effect on power generation.....	46
7 Conclusion and recommendations .....	49
References.....	50
Appendix.....	52

## List of Figures

Figure 1: CubeSat sizes [3] .....	1
Figure 2: Body-mounted solar arrays; CP8 IPEX (Cal Poly Intelligent Payload Experiment, app. 10 cm × 10 cm × 10 cm), RACE (Radiometer Atmospheric CubeSat Experiment)[10]...3	3
Figure 3: a) 12 solar panels configuration b) skirt solar panel configuration c) side and top solar panels configuration [11] .....	3
Figure 4: Eccentricity of an orbit [12] .....	4
Figure 5: Orbital elements [14].....	5
Figure 6: different solar arrays configurations [17].....	7
Figure 7: Deployed solar panels' geometrical configurations [9].....	8
Figure 8: The two phases of the deployment sequence [9].....	8
Figure 9: 3U CubeSat in orbit with a) free-orientation, b) sun pointing, and c) Nadir pointing [16].....	9
Figure 10: space-draft configuration [15]. .....	9
Figure 11: The Standard 3U CubeSat dimensions and 3U CubeSat with XSAS dimensions [18]. .....	10
Figure 12: a) Dual Panel design, b) Square design and c) Blanket deployable design [19]... 10	10
Figure 13: a) First design, b) Second design (partially deployed) and c) Second design (fully deployed).....	11
Figure 14: Final OPEN design.....	11
Figure 15: Methodology flow chart .....	12
Figure 16: Euler angles .....	14
Figure 17: CubeSat coordinates, Sun coordinates, and sun vector .....	15
Figure 18: 2U CubeSat [22].....	18
Figure 19: 3U CubeSat with 90 deployable solar panels. Note : the figure is generated using CubeSat Toolbox in MATLAB. ....	19
Figure 20: 3U CubeSat with 45-degree deployable solar panels. Note : the figure is generated using CubeSat Toolbox in MATLAB.....	20
Figure 21: 3U CubeSat model from STK .....	21
Figure 22: 3U CubeSat model from STK .....	21
Figure 23: power generation comparison in one day for 90-degree deployment angle model22	22



Figure 24: power generation comparison in two orbits for 90-degree deployment angle model .....	23
Figure 25: average power generation per orbit comparison in one day for 90-degree deployment angle model .....	23
Figure 26: power generation comparison in one day for 45-degree deployment angle model	23
Figure 27: power generation comparison in two orbits for 45-degree deployment angle model .....	24
Figure 28: average power generation per orbit comparison in one day for 45-degree deployment angle model .....	24
Figure 29: CubeSat toolbox analysis model .....	25
Figure 30: power generation comparison in one day for CubeSat Toolbox model .....	26
Figure 31: power generation comparison in two orbits for CubeSat Toolbox model .....	27
Figure 32: average power generation per orbit comparison in one day for CubeSat Toolbox model .....	27
Figure 33: Model1's solar panels configurations .....	29
Figure 34: Model2's solar panels configurations .....	29
Figure 35: power generation in two orbits for BMP-V .....	31
Figure 36: average power generation per orbit in one day for BMP-V .....	31
Figure 37: power generation in two orbits for BM-DP-V-90 .....	32
Figure 38: average power generation per orbit in one day for BM-DP-V-90 .....	32
Figure 39: power generation in two orbits for BM-DP-V-45 .....	32
Figure 40: average power generation per orbit in one day for BM-DP-V-45 .....	33
Figure 41: power generation in two orbits for DP-V-90 .....	33
Figure 42: average power generation per orbit in one day for DP-V-90 .....	33
Figure 43: power generation in two orbits for DP-V-45 .....	34
Figure 44: average power generation per orbit in one day for DP-V-45 .....	34
Figure 45: power generation in two orbits for BMP-H .....	34
Figure 46: average power generation per orbit in one day for BMP-H .....	35
Figure 47: power generation in two orbits for BM-DP-H-90 .....	35
Figure 48: average power generation per orbit in one day for BM-DP-H-90 .....	35
Figure 49: power generation in two orbits for BM-DP-H-45 .....	36
Figure 50: average power generation per orbit in one day for BM-DP-H-45] .....	36
Figure 51: BM-DP-V-90 solar vector plot .....	38

Figure 52: BM-DP-V-90 shadowed area. ....	39
Figure 53: BM-DP-V-90 raytracing in winter solstice .....	39
Figure 54: BM-DP-V-90 raytracing in vernal equinox.....	40
Figure 55: BM-DP-V-90 raytracing in summer solstice.....	40
Figure 56: BM-DP-V-90 raytracing in autumnal equinox.....	40
Figure 57: BM-DP-V-45 raytracing in winter solstice .....	41
Figure 58: BM-DP-V-45 raytracing in vernal equinox.....	41
Figure 59: BM-DP-V-45 raytracing in summer solstice.....	42
Figure 60: BM-DP-V-45 raytracing in autumnal equinox.....	42
Figure 61: BM-DP-H-90 raytracing in winter solstice .....	43
Figure 62: BM-DP-H-90 raytracing in vernal equinox.....	43
Figure 63: BM-DP-H-90 raytracing in summer solstice.....	43
Figure 64: BM-DP-H-90 raytracing in autumnal equinox.....	44
Figure 65: BM-DP-H-45 raytracing in winter solstice .....	44
Figure 66: BM-DP-H-45 raytracing in vernal equinox.....	45
Figure 67: BM-DP-H-45 raytracing in summer solstice.....	45
Figure 68: BM-DP-H-45 raytracing in autumnal equinox.....	45
Figure 69: BM-DP-V-90 power generation in one day with considering the self-shadowing	47
Figure 70: BM-DP-V-90 power generation in two orbits with considering the self-shadowing .....	47
Figure 71: Average power generation per orbit in one day for BM-DP-V-90 with considering self-shadowing .....	47
Figure 72: BM-DP-V-45 power generation in one day with considering the self-shadowing	48
Figure 73: BM-DP-V-45 power generation in two orbits with considering the self-shadowing .....	48
Figure 74: Average power generation per orbit in one day for BM-DP-V-45 with considering self-shadowing .....	48

## List of Tables

Table 1: Summarized results of Power generation code, STK and CubeSat Toolbox. ....	26
Table 2: Summary of Model1 and Model2 results .....	30
Table 3: Results of power generation considering self-shadowing .....	46

## List of Abbreviations

CDS	CubeSat standard design
CDS	CubeSat Design Specification
P-POD	Poly Picosatellite Orbital Deployer
EPS	CubeSat are Electrical power system
ADCS	Attitude Determination and Control System
OBC	Communications System, and On-Board Computer
PCB	Printed Circuit Boards
COTS	Commercial Off-The-Shelf
RAAN	Right ascension of the ascending node
XSAS	extendable solar array system
GMAT	General Mission Analysis Tool software
MATLAB	Matrix Laboratory software.
DCM	Direction Cosine Matrix
STK	Satellite Tool Kit

## List of Symbols

$a$	Semi-major axis
$e$	Eccentricity
$i$	Inclination
$\omega$	Argument of Perigee
$\nu_0$	True anomaly
$\psi$	yaw angle
$\theta$	pitch angle
$\phi$	roll angle

# 1 Introduction

## 1.1 Background

### CubeSat

A CubeSat is a nonmetric satellite that is mainly used for research and commercial applications. It was developed in 1999 as a project by California Polytechnic state university (CalPoly) and the Stanford University. The intention of this project is to facilitate access to space for small payloads, reduce the development cost and time, and sustain frequent launches by developing the CubeSat standard design (CDS).

The CubeSat is made up from one ( $10 \times 10 \times 10 \text{ cm}^3$ ) unit or multiple units in which each weight almost 1.3 kg as shown in Figure 1. It comprises of both systems and the payload inside the structure which are designed to meet the mission requirements and follow the CubeSat Design Specification (CDS). CubeSat is launched as a secondary payload in Poly Picosatellite Orbital Deployer (P-POD) which confirms the security of the CubeSat, primary payload of the launch vehicle, and other CubeSats[1,2] .

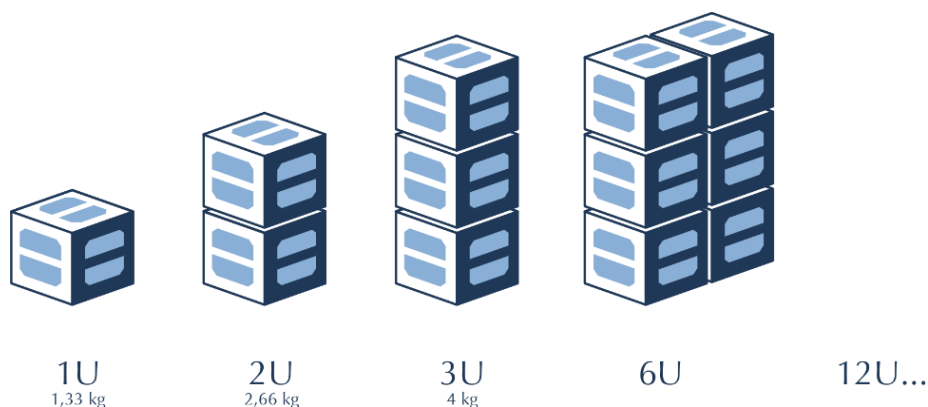


Figure 1: CubeSat sizes [3]

Like traditional satellites, the systems used in the CubeSat are Electrical power system (EPS), Attitude Determination and Control System (ADCS), Communications System, and On-Board Computer (OBC) which are essential to keep the satellite on orbit. These Systems mainly consist of Printed Circuit Boards (PCB) as a base line structure and build of Commercial Off-The-Shelf (COTS) components for the electronics which makes CubeSats available, low cost and consumes low power.[4]

## Power generation

The electric power system (EPS) manages the power generation, storage, and distribution on the CubeSat. Solar power generation is the most common method of power generation on CubeSats where the solar panels convert the incident solar energy into electrical energy [5].

While in orbit, a CubeSat is exposed to intervals of daylight and eclipse. The solar panels performance is a function of the incident solar intensity on the panel which varies during the orbit [6]. During the daylight period, a CubeSat is exposed to direct sunlight which allows the solar panels to generate the maximum electric power powering the CubeSat and charging the battery. Whereas in eclipse, the solar intensity is zero which indicates that there will be no power generation from the solar panels and instead the battery is used to power the CubeSat [7].

There are two approaches in designing the solar array system of a CubeSat, body-mounted solar arrays, and deployable solar arrays. In the body-mounted approach, the solar arrays are connected to the body of the satellite covering the whole structure whereas in the deployable design, the solar panels are attached to a planar structure where they are able to be deployed [8].

The CubeSat abilities could be improved by increasing the available power. By considering the specification and limitation of size and mass of a CubeSat, a deployable solar arrays system has been developed to increase the available on-board power [9].

### **Body-mounted solar arrays:**

The body-mounted solar arrays are installed directly on the satellite's structure. They are commonly used in small structures and missions with less than 2 kW power requirements [10]. This includes CubeSats. The advantages of using body-mounted solar arrays on CubeSat is the lack of deployment and tracking mechanisms which results in the simplicity of the design. One disadvantage is the limitation of the solar panels' coverage to the CubeSat's size. The orientation of the solar panels in this design with respect to the sun depends on the orientation of the CubeSat. Figure 2 shows two examples for body-mounted solar arrays [10].

According to C. Clark et al. [11], for a basic 1U CubeSat, the average power generation in a sun synchronous orbit with maximum eclipse period is no more than 1.9 Watt. Whereas, for a

standard 3U CubeSat, with nadir pointing (pointing to Earth) in the same orbital conditions, the average power generation is approximately 4.5 Watt [11].

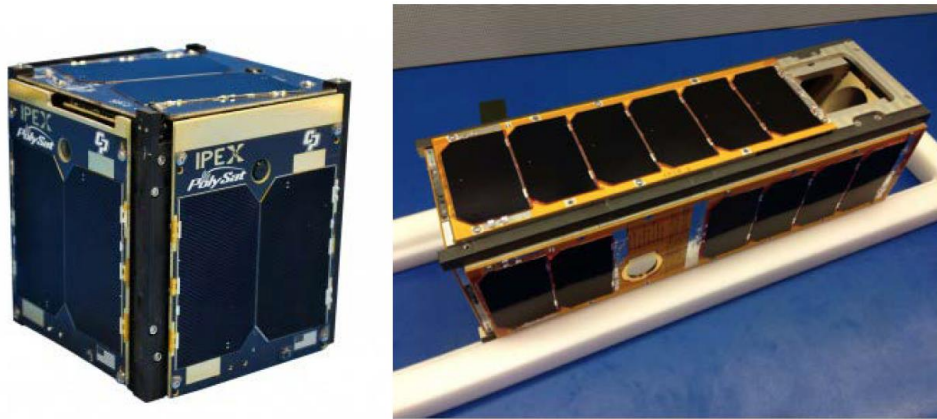


Figure 2: Body-mounted solar arrays; CP8 IPEX (Cal Poly Intelligent Payload Experiment, app. 10 cm × 10 cm × 10 cm), RACE (Radiometer Atmospheric CubeSat Experiment)[10].

### Deployable solar arrays:

The space solar arrays nowadays are deployed in space by using rigid panels with solar cells installed on a single side. These panels are attached to the satellite structure during the launch and upon deployment, they start unfolding from the structure [10].

Recently, CubeSats' generated power had been improved by developing new deployable solar arrays system designs. The simplest configuration is by using single solar array connected to the CubeSat's structure by one hinge. The more connected solar panels makes the configuration more complex.[9]

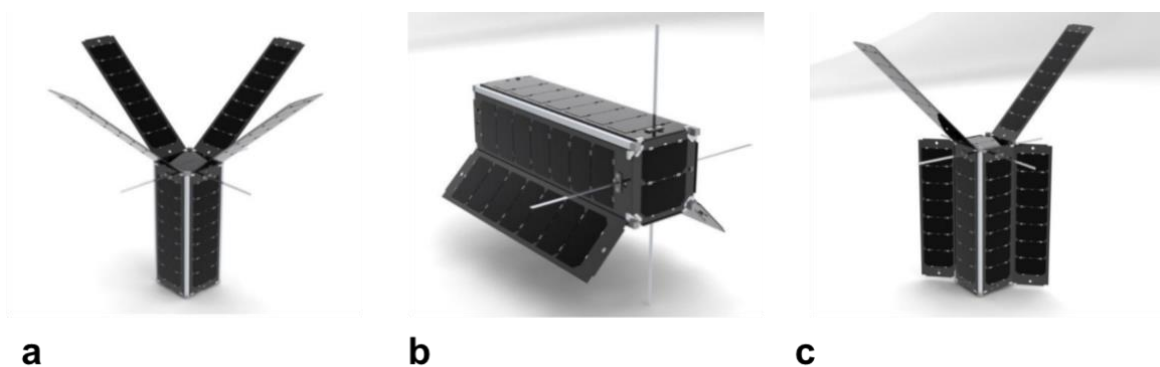


Figure 3: a) 12 solar panels configuration b) skirt solar panel configuration c) side and top solar panels configuration [11]

As mentioned in the previous study by C. Clark et al. [11], for a standard 3U CubeSat with 4 body-mounted solar panels and 4 deployable double sided solar panels (Figure 3-a), in a sun synchronous orbit with maximum eclipse, the power generation has been increased to 11.7 Watt. Whereas for the 3U skirt solar panel configuration (Figure 3-b), the average power is 6.6



Watt. And finally, for the side and top deployed solar panel configuration (Figure 3-c), the average power generation is 18.9 Watt [11].

## Orbit definition

The motion of a satellite around the Earth and along its orbit can be described by six Keplerian or classical orbital elements of an elliptical orbit.

The classical orbital elements are (Figure 5):

- **Semi-major axis ( $a$ )** is the half distance across the long axis of the ellipse, it describes size of the orbit.
- **Eccentricity ( $e$ )** describes the shape of the orbit as shown in Figure 4 (0=circle,  $<1$ =ellipse,  $1$ = parabola,  $>1$ =hyperbola)
- **Inclination ( $i$ )** is the angle between the equator plane of the Earth and the orbit plane.
- **Right ascension of the ascending node (RAAN)** is the angle measured between the ascending node and the vernal equinox in the equatorial plane.

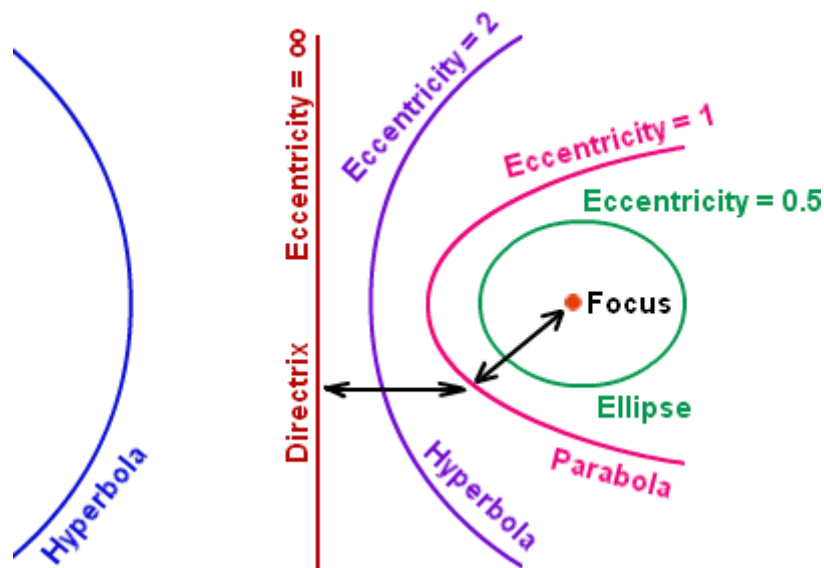


Figure 4: Eccentricity of an orbit [12]

The ascending node is the node where the spacecraft cross the equatorial plane going from south to north. And the vernal equinox is the point where the Earth crosses the Earth-Sun ecliptic plane on the first day of spring.

- **Argument of Perigee ( $\omega$ )** is the angle between the ascending node and the Perigee in the orbital plane. The Perigee which is the point where the satellite becomes closest to Earth.

The Apogee is the most distant point from Earth. Both Perigee and Apogee are in the orbital semi-major axis direction.

- **True anomaly ( $v_0$ )** is the angle in the orbital plane measured from the Perigee to the satellite [13].

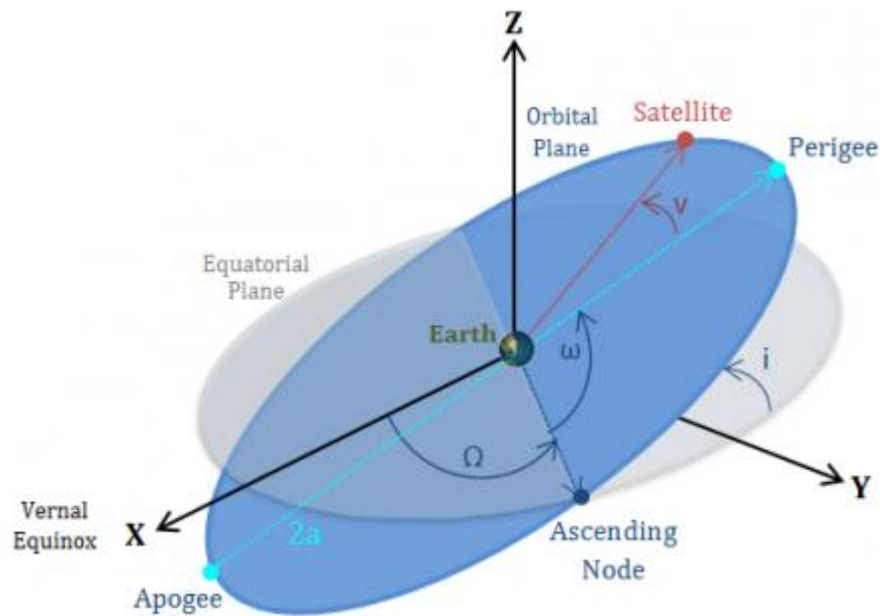


Figure 5: Orbital elements [14]

## 1.2 Problem Statement and Research Objectives

Today, CubeSats are common for military, commercial and scientific research missions due to their low development costs and standardized form factors compared to large satellites. However, the available on-board power is limited in CubeSats because of the limitation in the solar panels area and the eclipse environment. In CubeSats, deployable solar arrays system is used to increase the power generation. This can enhance the CubeSat's performance and the mission's scenarios available for the small satellites.

The deployable solar arrays could be designed in various shapes, directions, and angles as shown in Figure 6 in order to maximize the power. There are factors that affects the designs of the deployable solar arrays which are the repeated encounters with Earth's shadow and the time-varying, highly dynamic direction vectors from Satellite to the Sun [11,15,16].

In order to reach the optimum design, it is important to find expressions for the power generated as a function of the orbital elements and CubeSat pointing scenario. To validate such expressions, it necessary to apply them to actual CubeSat missions. This includes the determination of the power demand throughout the Satellite mission. This should be carried out based on an analysis that accounts for the mission phases, the orbit parameters, and the performance degradation.

The objectives of this research are the following:

- Edit and modify the power generation code that is used in YahSat Space Lab.
- Verify the validity of the code.
- Find the power generation of different models with different solar panels configurations of a 3U CubeSat in Low Earth Orbit.
- Estimate the self-shadowing effect on the proposed models.

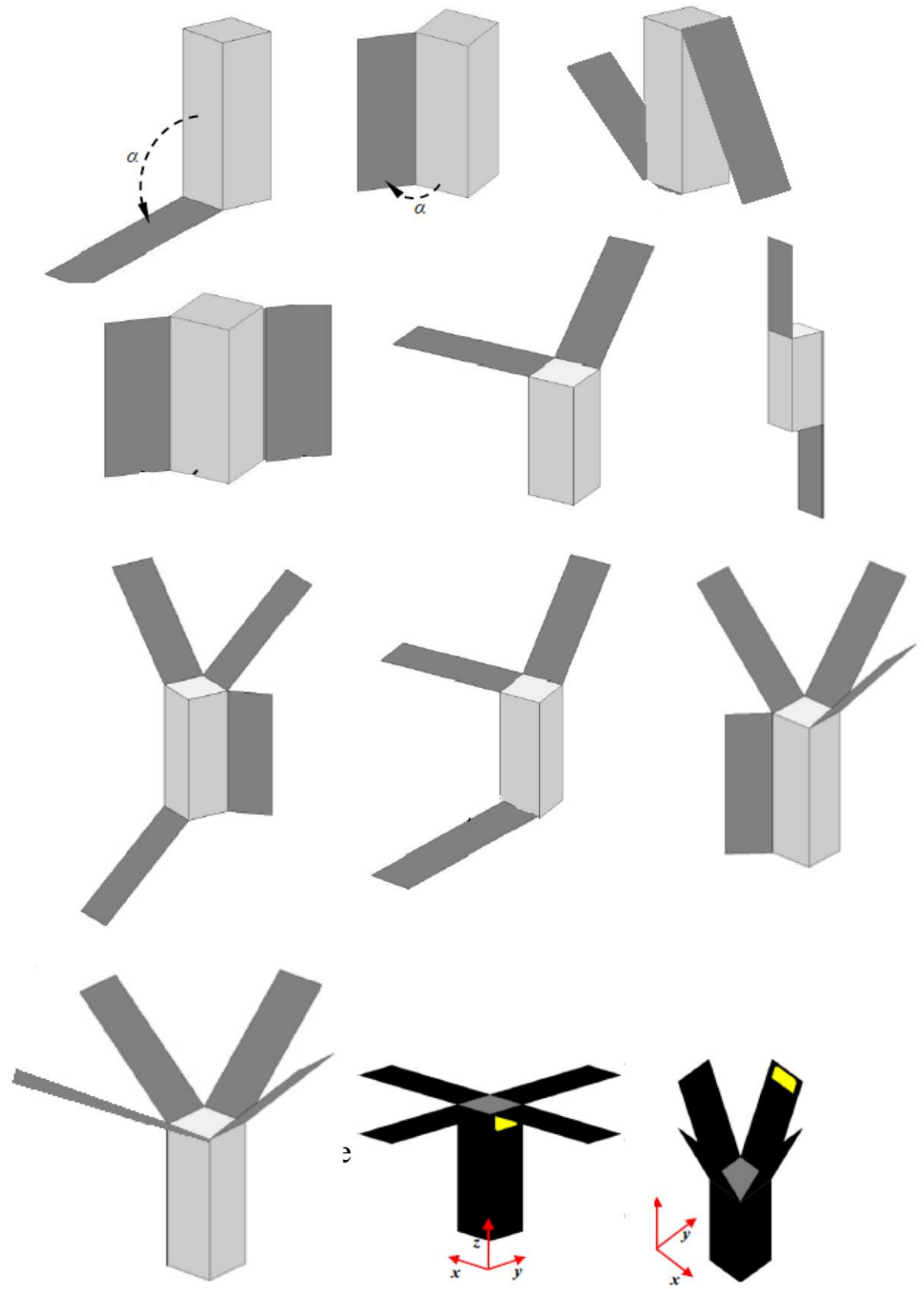


Figure 6: different solar arrays configurations [17].

## 2 Literature Review

The solar array performance depends on many factors such as position of the sun in different seasons, orbit, attitude, and the geometric design. A study by F. Santoni et al. [9] had been developed to analyze these factors where a design analysis was devoted to compare the performance of the fixed and steerable deployed solar panel in circular sun-synchronous orbits assuming nadir pointing for the satellite attitude, which results into using the steerable solar panel system because it has a higher performance. A design trade-off has been conducted on two deployment architecture configurations which are illustrated in Figure 7, the longitudinal configuration has been selected based on the aspects it has compared to the lateral. The deployment sequence is developed in two steps as indicated in Figure 8. A deployable solar panel design and prototype has been done based on the above configurations and the requirement specified for the CubeSat for the deployment sequence ground testing which has been performed for several times without any failure or major problems.

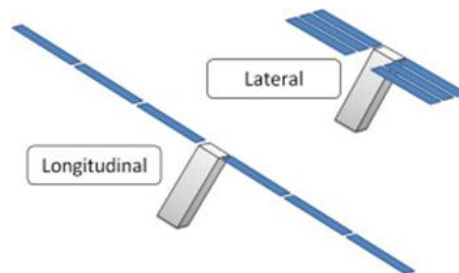


Figure 7: Deployed solar panels' geometrical configurations [9].

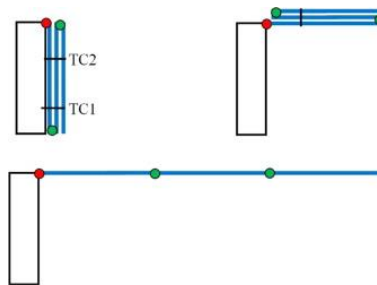


Figure 8: The two phases of the deployment sequence [9].

Another study by Sanchez-Sanjuan et al. [16] had focused on the importance of estimating the incident solar energy on a CubeSat as a function of the orbital parameters and the altitude during the designing phase. Kinematic and dynamic equations of the CubeSat attitude had been described. In addition, the mathematical models were derived to calculate the energy harvest by the solar panels and energy stored in the battery. These models were applied on a 3U CubeSat with body-mounted solar panels considering three scenarios: nadir-pointing, sun-

pointing, and free-pointing scenarios as shown in Figure 9. The results of this study indicated that free-orientation and Sun-pointing scenarios harvest extra power than nadir-pointing scenario.

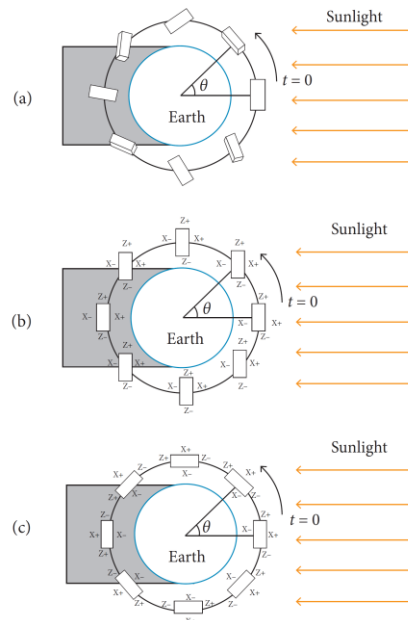


Figure 9: 3U CubeSat in orbit with a) free-orientation, b) sun pointing, and c) Nadir pointing [16].

In a recent study by Young Lee et al. [15] introduced different objective functions to be applied based on the satellites design which is used for energy management. In this study, they developed an algorithm to be used in finding the optimal panel angles which maximize power generation using a power generation model, also they designed a simulation system to apply the objective function and in addition to that, they developed a technique to assess shadow-induced power reduction in complex configurations and finally applying the above to a space-draft configuration shown in Figure 10 to find the optimal solar panel deployment angles that maximize total power generation under different orbit conditions.

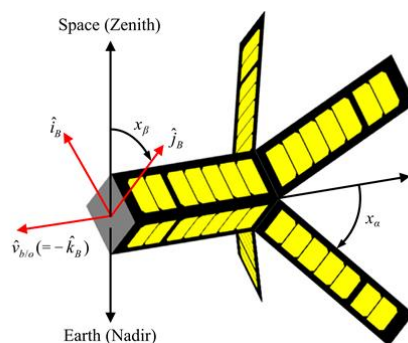


Figure 10: space-draft configuration [15].

A novel design for the solar array was illustrated in a study by P. Senatore et al. [18]. An extendable solar array system (XSAS) was designed to maximize the power available for the CubeSat. This system consists of 14 solar panels that are stowed in the half of the 3U structure as shown in Figure 11. XSAS provides an average power of 23W and a maximum power of 32W. A prototype was created to demonstrate the high-risk mechanisms of the system.

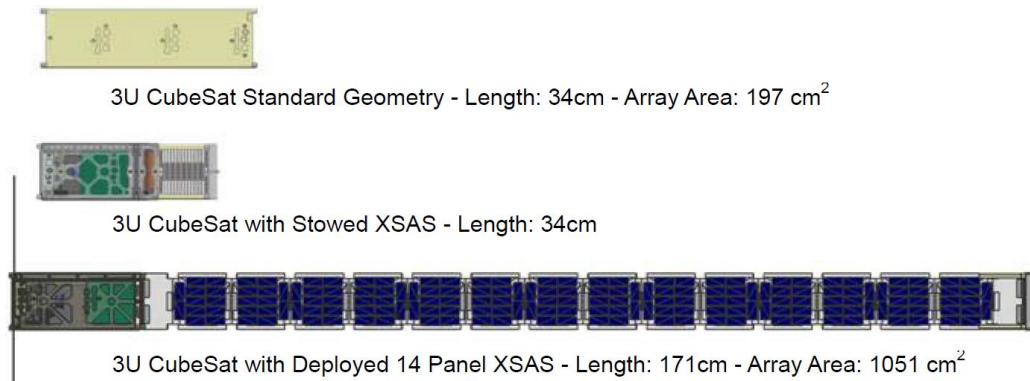


Figure 11: The Standard 3U CubeSat dimensions and 3U CubeSat with XSAS dimensions [18].

Another study by B. Kading et al. [19], focuses on an important factor in designing spacecraft which is the longevity. This paper provides us with multiple novel deployable solar array designs that will enhance the longevity of the spacecraft. Three designs were introduced: Dual Panel design, Square design and Blanket deployable design as shown in Figure 12. Mass, volume and qualitative analysis had been conducted and it shows that all the designs increases the longevity by different factors. The blanket has the highest effect, it increases the longevity by 8 times.

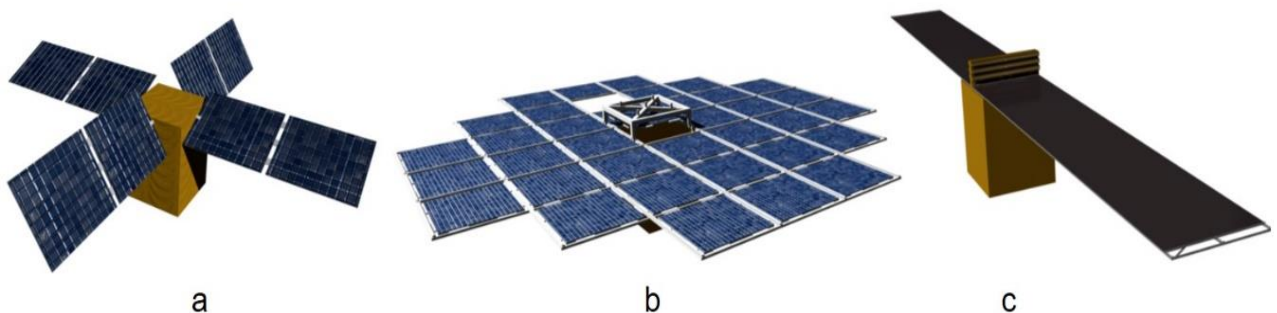
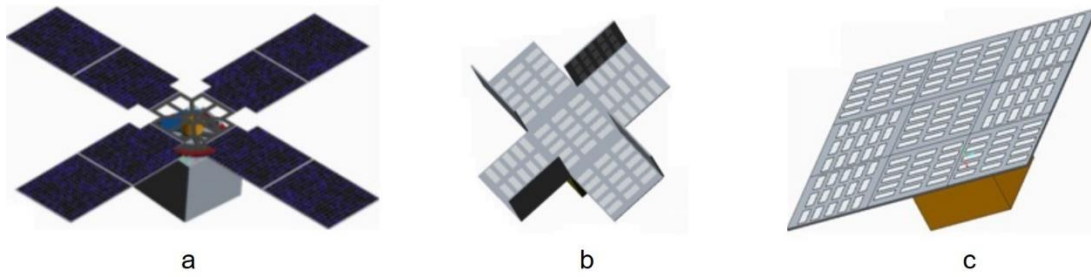


Figure 12: a) Dual Panel design, b) Square design and c) Blanket deployable design [19].

1U Deployable solar panel system was designed in a study for OPEN CubeSat [20]. A trade off study between two available designs (Figure 13) with two phase deployment system has

been conducted. Due to the mass and volume limits for a 1U CubeSat and the high complexity of the deployment system, the design was reduced as shown in Figure 14. The power generation increased in this design in the optimal orientation by 235.8%.



*Figure 13: a) First design, b) Second design (partially deployed) and c) Second design (fully deployed)*

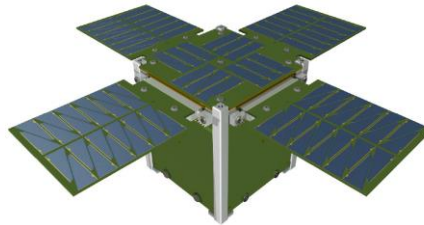


*Figure 14: Final OPEN design*



### 3 Methodology

in this chapter, the methodology of estimating the power generated by a CubeSat in orbit is briefly explained in terms of defining the orbit, simulating it using the General Mission Analysis Tool (GMAT) software, and finally computing the power generation using Matrix Laboratory (MATLAB) software.

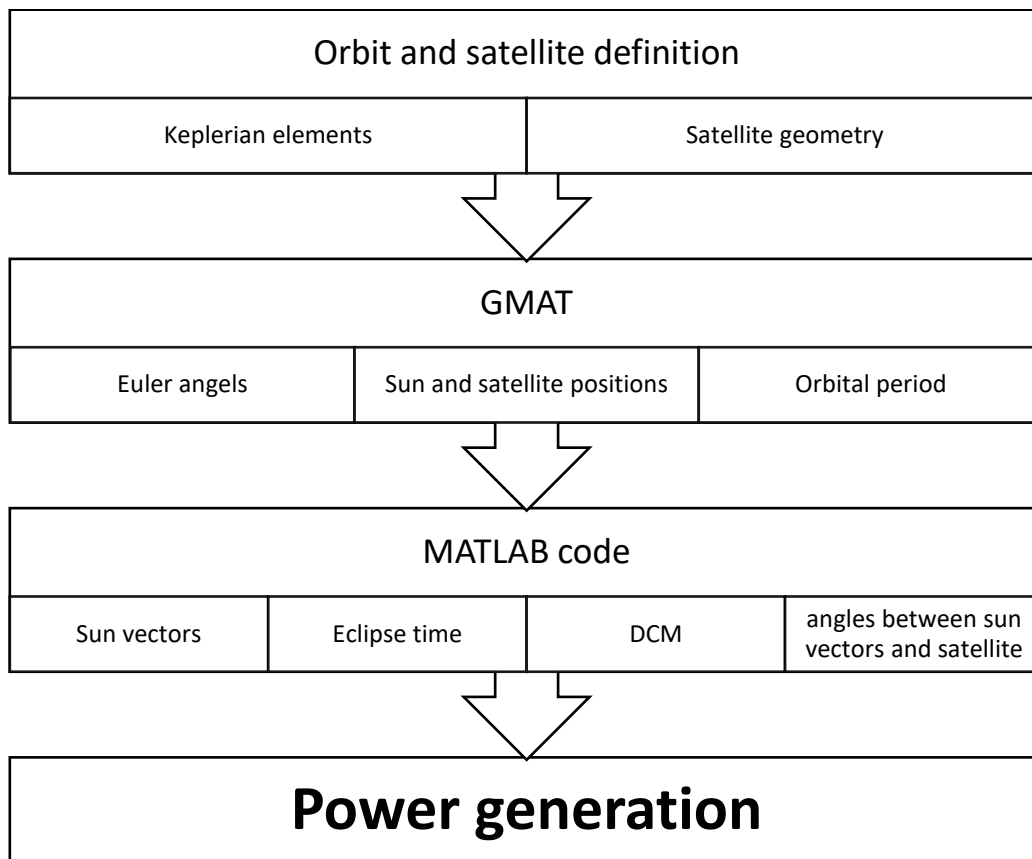


Figure 15: Methodology flow chart

The research methodology overview is shown in Figure 15. First, the CubeSat’s mission should be defined in terms of size and orbit. Second, the CubeSat’s parameters will be entered in General Mission Analysis Tool (GMAT) software which will simulate the orbit of the CubeSat and extract the Euler angles, sun, and satellite positions with respect to Earth and the orbital period. Third, these data will be used in an algorithm created in Matrix Laboratory (MATLAB)

software to compute the sun vectors from the CubeSat to the sun, eclipse time, Direction Cosine Matrix (DCM) and the angles between the sun vectors and the satellite. Finally, based on the CubeSat geometry and solar panel power parameters, the power generated is calculated.

### **3.1 Orbit and satellite definition**

The first step of the analysis is to define the data input in GMAT software. These data consist of the CubeSat's specifications and Keplerian orbital elements. The CubeSat's data includes CubeSat's model, mass, drag coefficient, and CubeSat attitude which could be nadir pointing, spinning or sun pointing.

The Keplerian orbital elements should be defined based on the mission requirements. These elements are: Semi-major axis ( $a$ ), inclination ( $i$ ), eccentricity ( $e$ ), right ascension of the ascending node (RAAN), true anomaly, and argument of perigee. The Keplerian elements describes the orbital plane, orbit size, and the satellite's position.

In this project, a 3U CubeSat model with nadir pointing attitude will be analysed based on the missions that space lab is working on. Different solar panel configurations will be studied to find the best configuration for such attitude that provides the maximum power. The orbit will be LEO with a 400 km altitude.

### **3.2 Orbit simulation**

To simulate the orbit of the CubeSat around the Earth, General Mission Analysis Tool (GMAT) software is used. First, an Epoch time should be defined in GMAT in addition to the previously mentioned data.

The Epoch time is defined as 20 Mar 2021 08:00:00 UTCG. The semi-major axis is 6771km, inclination is 51.6 and eccentricity is zero. The attitude of the CubeSat is nadir pointing towards Earth in negative Z direction and constrained with the velocity in X direction where X direction

will be always in the direction of the motion of the satellite along its orbit. Other parameters should be as default setup of the software. These conditions were choose based on the previous missions' parameters in the space lab.

Form this simulation, the following data are extracted at every time step during the orbit:

- Euler angels (represent the Roll  $\varphi$ , Yaw  $\psi$ , and Pitch  $\theta$  angles of the CubeSat with respect to the Earth frame)

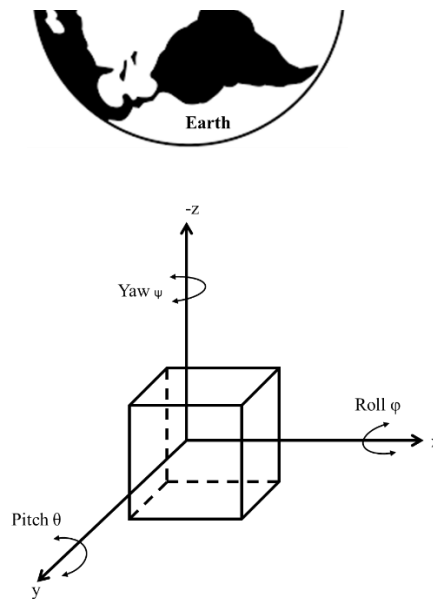


*Figure 16: Euler angles*

- Sun position coordinates with respect to Earth frame.
- CubeSat position coordinates with respect to Earth frame.
- Eclipse times

### 3.3 Power generation calculations

A MATLAB code was created by engineer Alexandros Tsoupos and edited by me and my colleagues Rzan Al-Haddad and Nouf Alzaabi is used to compute the power generated from the CubeSat solar panels. The MATLAB code starts by importing the extracted GMAT data and compute the number of nodes based on time step of the extracted data.

First, the Sun vector which is the vector from the CubeSat to the Sun is calculated by subtracting the CubeSat coordinates from Sun coordinates that are obtained by GMAT as shown in Figure 17. The Sun vector then is normalized by dividing it by the magnitude.

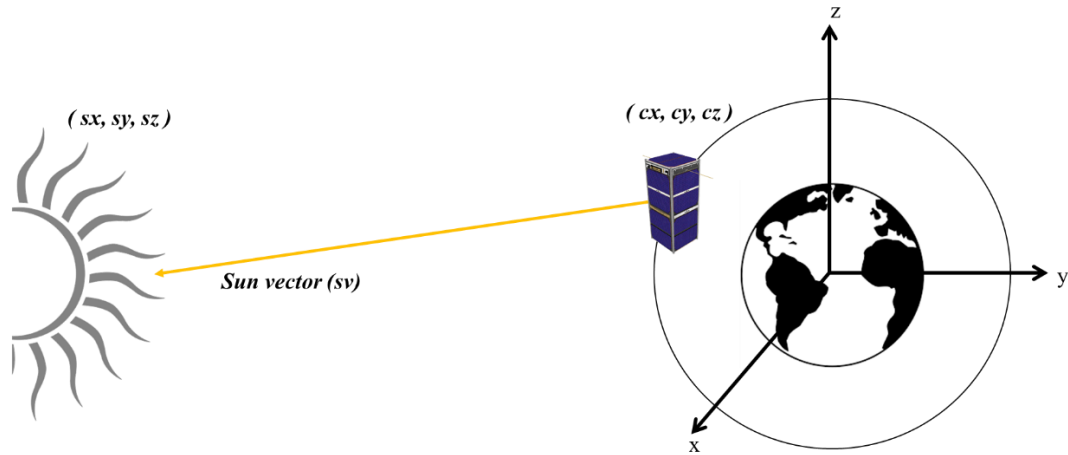


Figure 17: CubeSat coordinates, Sun coordinates, and sun vector

$$sv = \begin{bmatrix} sx - cx \\ sy - cy \\ sz - cz \end{bmatrix} \quad 3.1$$

$$|sv| = \sqrt{(sx - cx)^2 + (sy - cy)^2 + (sz - cz)^2} \quad 3.2$$

$$sv = sv/|sv| \quad 3.3$$

Second, the code reads the Eclipse times file obtained by GMAT and assign the indexes that are during eclipse as eclipse indexes that will be used later.

Then, an identity matrix is generated which will be used to define the CubeSat body frame.

$$ux = [1 \ 0 \ 0] \quad 3.4$$

$$uy = [0 \ 1 \ 0] \quad 3.5$$

$$uz = [0 \ 0 \ 1] \quad 3.6$$

A Direction Cosine Matrix (DCM) is generated at every time step from the Euler angles obtained by GMAT using “angle2dcm” function. It uses the 321 sequence, which means the CubeSat orientation is obtained by rotating it around the Z-axis by yaw angle ( $\psi$ ). Then, it is

rotated around Y-axis by pitch angle ( $\theta$ ). Finally, it is rotated around X-axis by roll angle ( $\phi$ ).

The single rotation matrixes are:

$$R_1 = R_Z(\psi) = \begin{bmatrix} \cos \psi & \sin \psi & 0 \\ -\sin \psi & \cos \psi & 0 \\ 0 & 0 & 1 \end{bmatrix} \quad 3.7$$

$$R_2 = R_Y(\theta) = \begin{bmatrix} \cos \theta & 0 & -\sin \theta \\ 0 & 1 & 0 \\ \sin \theta & 0 & \cos \theta \end{bmatrix} \quad 3.8$$

$$R_3 = R_X(\phi) = \begin{bmatrix} 1 & 0 & 0 \\ 0 & \cos \phi & \sin \phi \\ 0 & -\sin \phi & \cos \phi \end{bmatrix} \quad 3.9$$

The Direction cosine matrix is found as:

$$DCM = R_3 R_2 R_1 = \begin{bmatrix} \cos \theta \cos \psi & \cos \theta \sin \psi & -\sin \theta \\ -\cos \phi \sin \psi + \sin \phi \sin \theta \cos \psi & \cos \phi \cos \psi + \sin \phi \sin \theta \sin \psi & \sin \phi \cos \theta \\ \sin \phi \sin \psi + \cos \phi \sin \theta \cos \psi & -\sin \phi \cos \psi + \cos \phi \sin \theta \sin \psi & \cos \phi \cos \theta \end{bmatrix} \quad 3.10$$

To transform the identity matrix to represent the body frame, it is pre-multiplied by the DCM.

$$ux(t) = DCM(t) * ux(t)^T \quad 3.11$$

$$uy(t) = DCM(t) * uy(t)^T \quad 3.12$$

$$uz(t) = DCM(t) * uz(t)^T \quad 3.13$$

Then, the projection of the sun vectors onto the CubeSat body frame are found by the dot product which will represent the CubeSat sides.

$$ax = ux . sx \quad 3.14$$

$$ay = uy . sy \quad 3.15$$

$$az = uz . sz \quad 3.16$$

These projections represent the effective area of each side of the CubeSat that is subjected to the solar radiation or can be thought of as the portion of the sunlight that is incident of each side of the CubeSat.

The sides of the CubeSat are defined based on their values. If it is positive, that means the side is in the positive side of the model and vice versa.

Also, they are defined as zero in the eclipse times which means there is no power generation in this particular time.

$$ax_+ = ax > 0 \quad 3.17$$

$$ax_- = ax < 0 \quad 3.18$$

$$a = [ax_+ \ ax_- \ ay_+ \ ay_- \ az_+ \ az_-] \quad 3.19$$

A new matrix is generated to define the model's body-mounted solar cells area. Based on the model, the users should identify how many solar cells are there on the CubeSat structure.

$$noc = (0.003031 \text{ m}^2) [x_+ \ x_- \ y_+ \ y_- \ z_+ \ z_-] \quad 3.20$$

Where 0.003031 is the area of one solar cell based on GomSpace solar panel's datasheet [21].

For instance, the Model shown in Figure 18 has 4 solar cells in positive X and negative X directions, 4 solar cells in positive Y and negative Y directions and 2 solar cells in positive Z and negative Z directions. So, the noc for this model is:

$$noc = (0.003031 \text{ m}^2) [4 \ 4 \ 4 \ 4 \ 2 \ 2] \quad 3.21$$

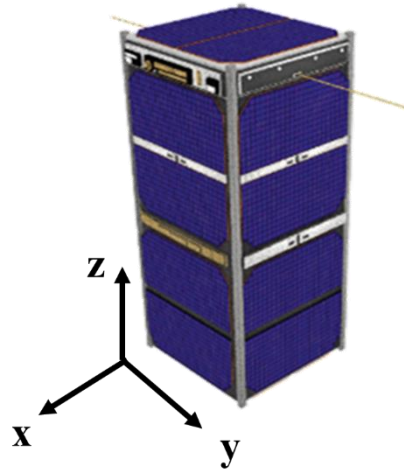


Figure 18: 2U CubeSat [22]

Finally, the power is calculated by multiplying the efficiency of the solar cells ( $\epsilon$ ), solar constant that is  $1376 \text{ w/m}^2$ , effective solar panels area ( $a$ ) and the transpose of the number of cells ( $noc^T$ ). The efficiency ( $\epsilon$ ) is considered to be 30% based on GomSpace solar panel's datasheet [21].

$$P = \epsilon * (1376 \text{ w/m}^2) * a * noc^T \quad 3.22$$

In the case of deployable solar arrays if the deployment angle is 90, nothing will need to be added to the code. Except that the user will identify more solar cells on the required side. For example, in the model shown in Figure 19 has 18 solar cells on the positive Z direction, 6 solar cells in negative Z, negative Y, and positive Y, and 2 solar cells in positive X and negative X directions.

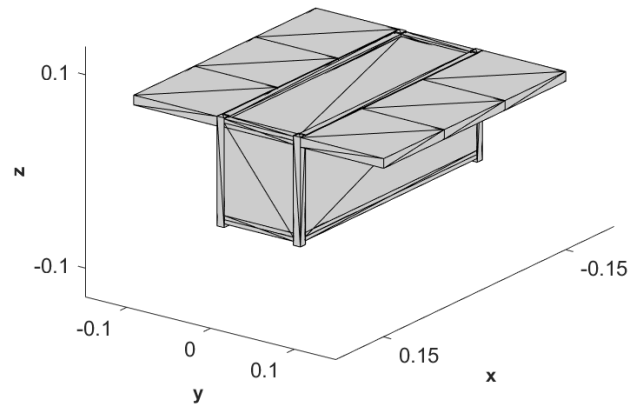


Figure 19: 3U CubeSat with 90 deployable solar panels. Note : the figure is generated using CubeSat Toolbox in MATLAB.

Other cases with other deployment angles than 90-degrees, another identity matrix for the deployable solar panel is made and another DCM is generated based on the deployment angle of the solar panel. The identity matrix will first be multiplied with the original DCM to transform them to the CubeSat body frame and then it is multiplied by the second DCM to transfer it to the local solar panel coordinates. Then, the sun vectors also are projected on the local solar panel coordinated and the number of solar cells is then identified for each wing. Finally, the power generation is calculated.

Taking Figure 20 as an example, two identity matrices will be defined. First, it is for the CubeSat body mounted solar panels. Second, it is for the two deployable solar panels



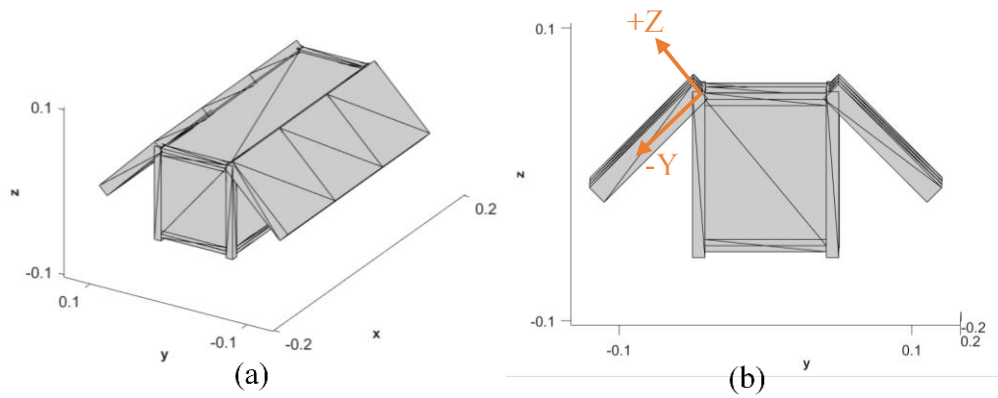


Figure 20: 3U CubeSat with 45-degree deployable solar panels. Note : the figure is generated using CubeSat Toolbox in MATLAB.

In this case, the second identity matrix will be transformed to the CubeSat body frame and then it is transferred again to the local solar panel coordinate by 45 degrees around the X axis of the CubeSat body frame. So the new coordinates are shown in Figure 20 (b) which indicates that there are six solar cells in positive Z direction and another six in positive Y direction to be identified to find the power.

## 4 Verification of the code

In this chapter, the results of the code are compared to two different references to validate the code. First, Satellite Tool Kit (STK) which is a physics-based software from Analytical Graphics that is offered for land, sea, air, and space systems to evaluate their performance in real time. Second, CubeSat Toolbox for MATLAB® is an educational product from Princeton Satellite Systems company for designing CubeSats and analyzing typical CubeSat missions.

### 4.1 STK results

The results were compared for two different solar panels configurations of a 3U CubeSat. The CubeSat model, analysis parameters and the results are discussed in this section.

#### CubeSat model

The standard 3U CubeSat from STK library was used with a 90-degree deployment angle and with nadir pointing in negative Z direction and it is aligned with the velocity in negative X direction as shown in Figure 21. The same model with different deployment angle also was used as shown in Figure 22.

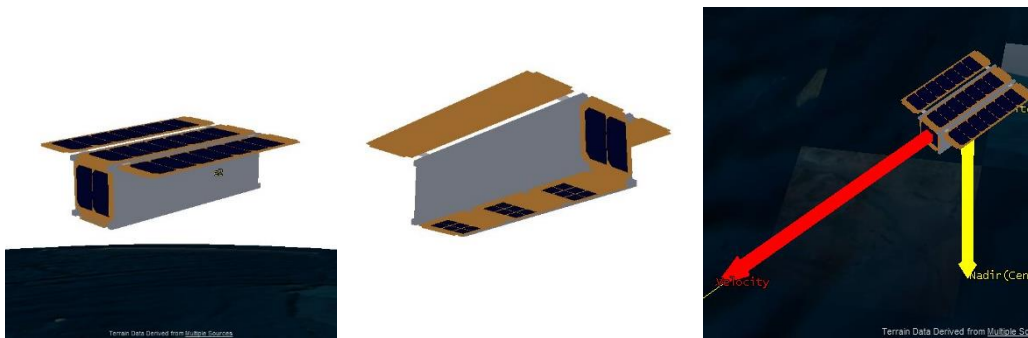


Figure 21: 3U CubeSat model from STK

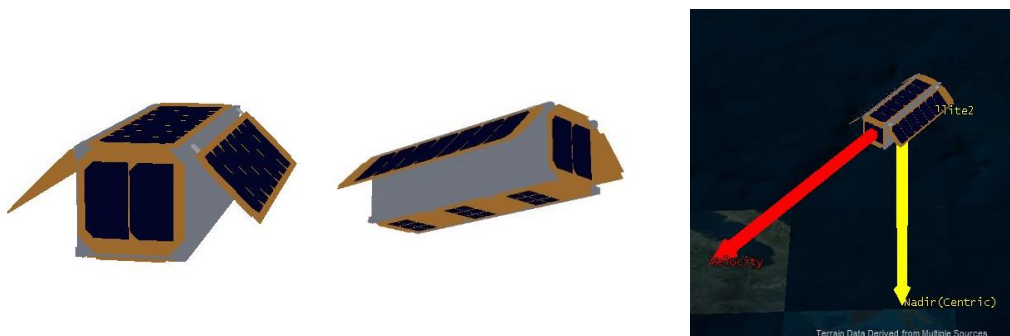


Figure 22: 3U CubeSat model from STK

## Analysis parameters

The analysis parameters are:

- Epoch time: 20 March 2021 at 08:00:00 UTCG
- Semi-major axis (a) = 6771 km
- Eccentricity (e) = 0
- Inclination (i) = 51.6
- Time step: 30 second for one day analysis's period.

## Analysis results

The results of the 90-degree deployment angle model shows that the average power in STK software is 7.75 W and from the code is 7.56W which is lower by 3%. The power generation by the solar panels throughout the orbit are compared in Figure 23 and Figure 24. The average power generation per orbit in one day are compared in Figure 25.

In addition, the results of the 45-degree deployment angle model show that the average power in STK software is 6.42 W and from the code is 6.2 W which is lower by 3.4%. The power generation by the solar panels throughout the orbit are compared in Figure 26 and Figure 27. The average power generation per orbit in one day are compared in Figure 28.

The figures for both 90-degree and 45-degree deployment angles models shows the same behaviour, the same eclipse duration, and with the same curve peaks. Even the average power generation figures have the same behaviour as shown in Figure 25 and Figure 28.

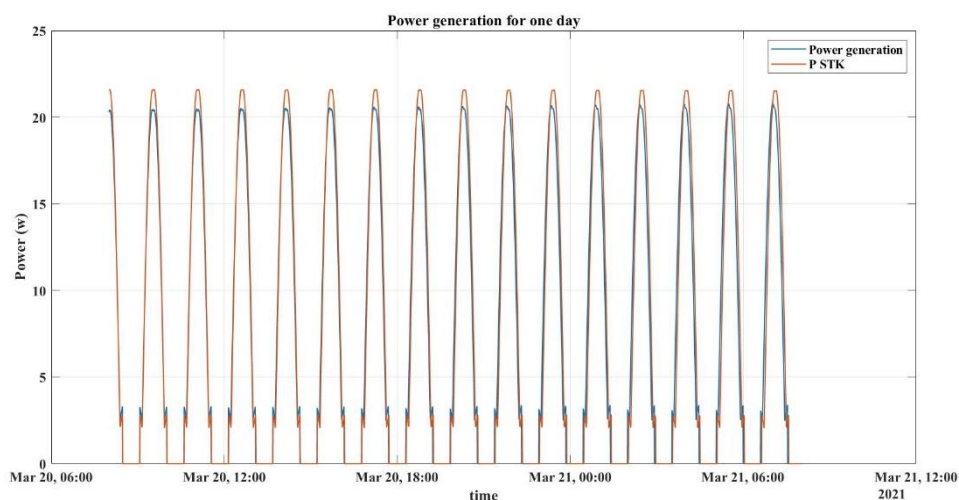


Figure 23: power generation comparison in one day for 90-degree deployment angle model

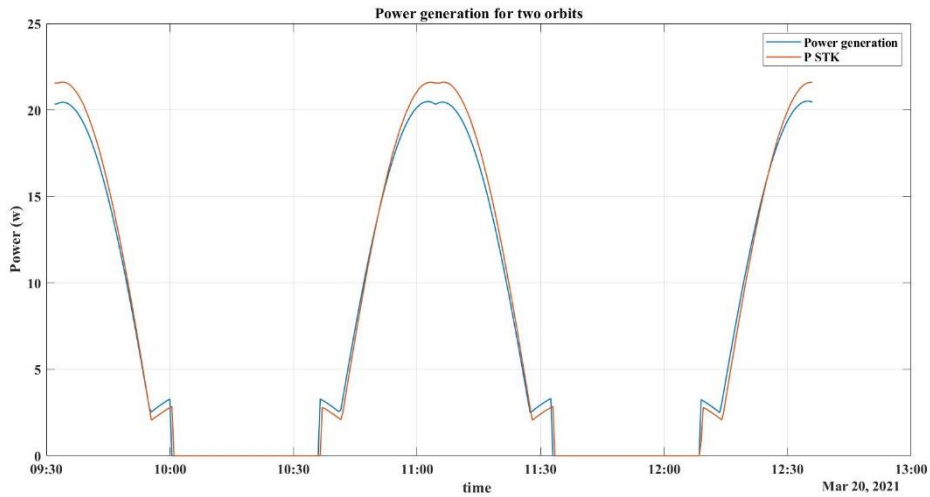


Figure 24: power generation comparison in two orbits for 90-degree deployment angle model

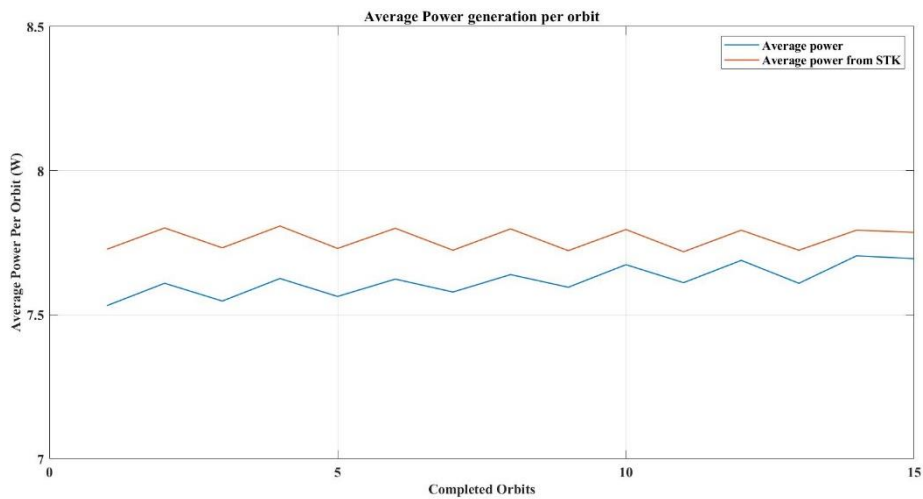


Figure 25: average power generation per orbit comparison in one day for 90-degree deployment angle model

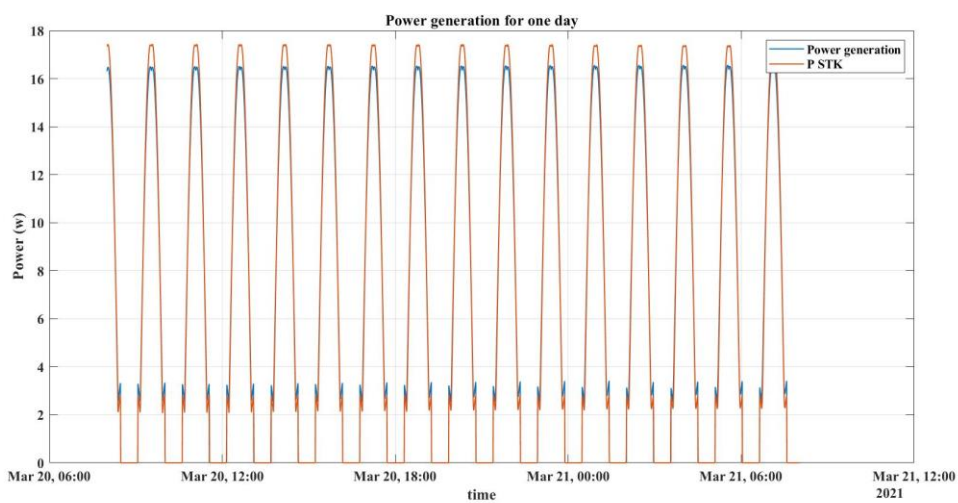


Figure 26: power generation comparison in one day for 45-degree deployment angle model

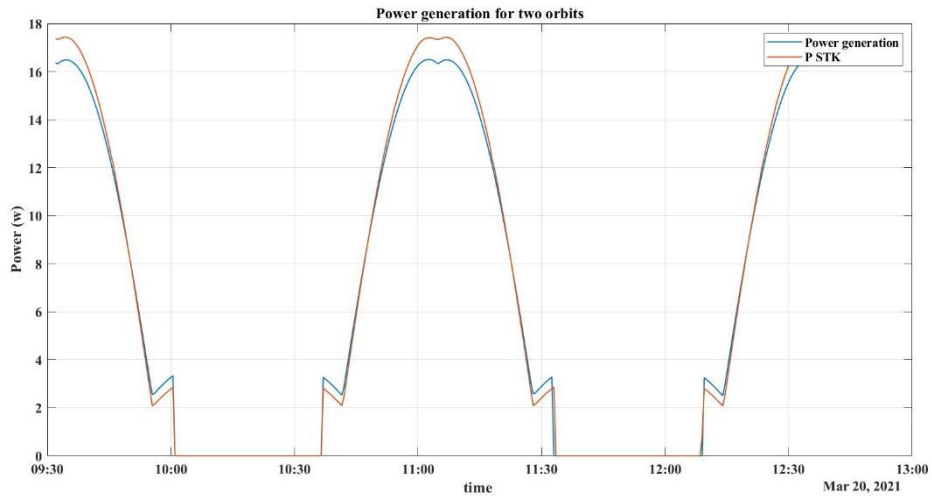


Figure 27: power generation comparison in two orbits for 45-degree deployment angle model

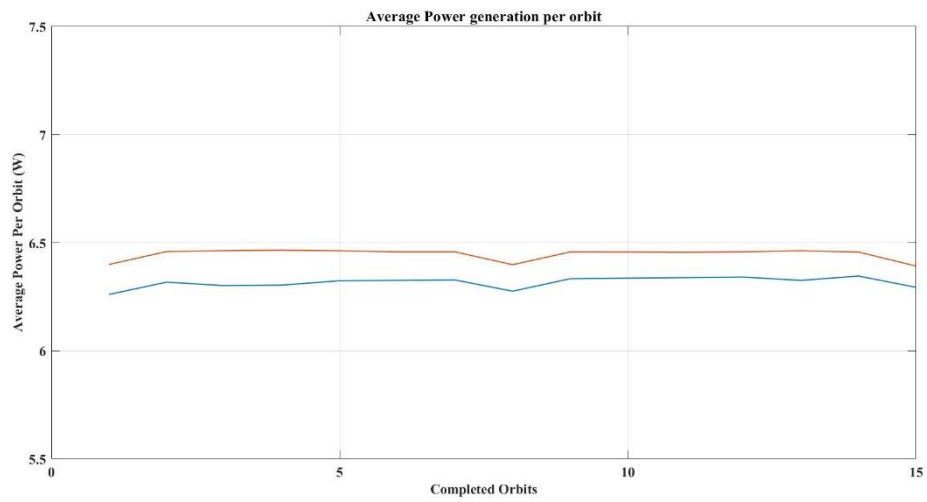


Figure 28: average power generation per orbit comparison in one day for 45-degree deployment angle model

## 4.2 CubeSat Toolbox results

In this section, the results of the code were compared to the results obtained from Princeton Satellite Systems CubeSat Toolbox code [23]. The CubeSat toolbox is a MATLAB toolbox to design CubeSats and analyze the mission. It consists of various functions and it has many demos for orbit simulation, power, mission planning, and thermal simulations. The CubeSat model, analysis parameters and the results are discussed in this section.

### CubeSat model

The same model of the standard 3U CubeSat from STK with a 90-degree deployment angle was used. The results were compared as well with the STK results. The model drawing is shown in Figure 29.

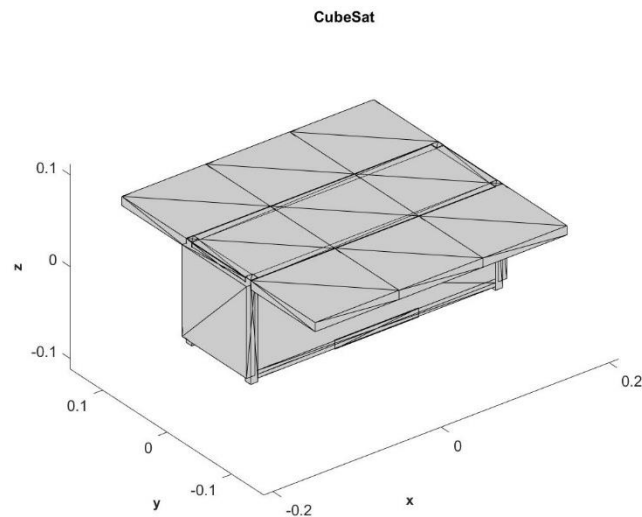


Figure 29: CubeSat toolbox analysis model

### Analysis parameters

The analysis parameters are:

- Epoch time: 20 March 2021 at 08:00:00 UTCG
- Semi-major axis ( $a$ ) = 6771 km
- Eccentricity ( $e$ ) = 0
- Inclination ( $i$ ) = 51.6
- Time step: 30 second for one day analysis.

## Analysis results

The results of the analysis show that the average power in STK software is 7.75 W and from the code is 7.56W which is lower by 3%. And from the CubeSat Toolbox is 8.15 W which higher than STK result by 5% and higher than the code result by almost 7%. The power generation by the solar panels from all the resources are compared in the following figures.

The figures below show the same behaviour for all STK, CubeSat Toolbox, and the power generation code. All the curves have the same eclipse duration, and with the same curve peaks. In addition, the average power curves in Figure 32 have the same behaviour.

The summarized results for all models are shown in Table 1.

Table 1: Summarized results of Power generation code, STK and CubeSat Toolbox.

Model	Power generation (W)		
	Power generation code	STK	CubeSat Toolbox
90-degree	7.56	7.75	8.15
45-degree	6.2	6.42	N/A

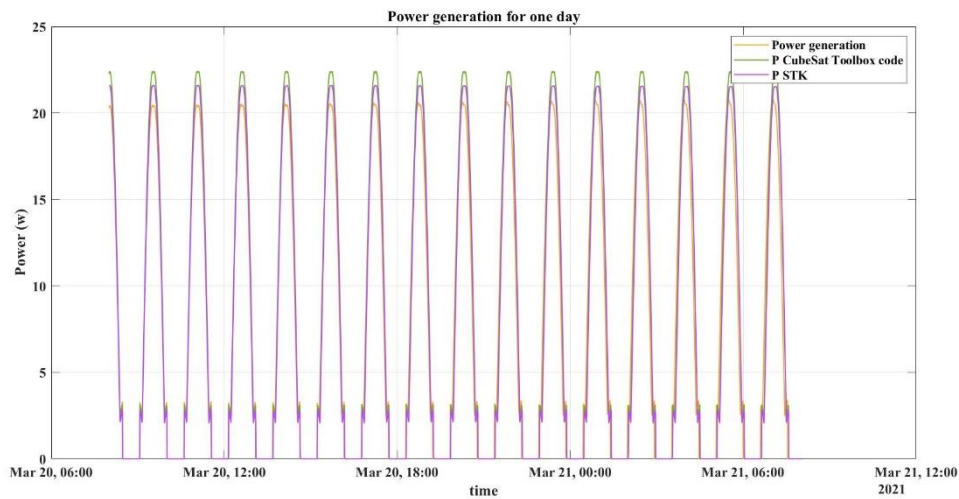


Figure 30: power generation comparison in one day for CubeSat Toolbox model

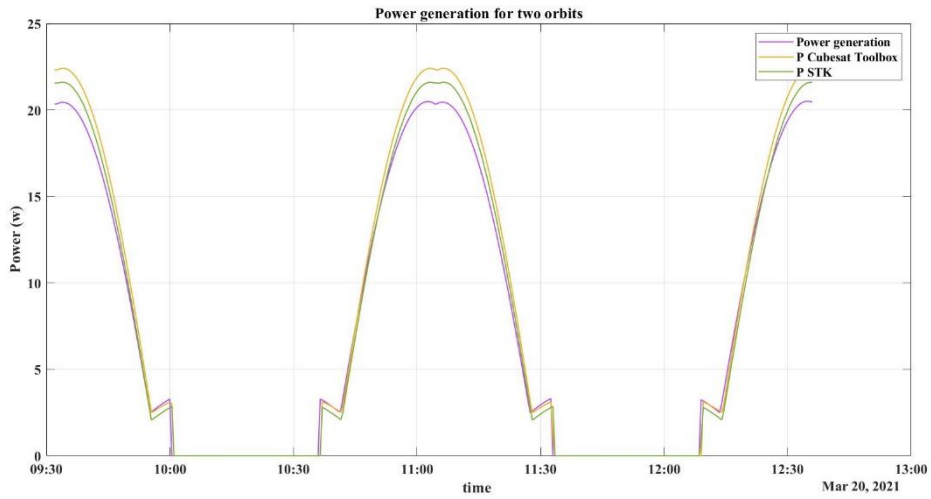


Figure 31: power generation comparison in two orbits for CubeSat Toolbox model

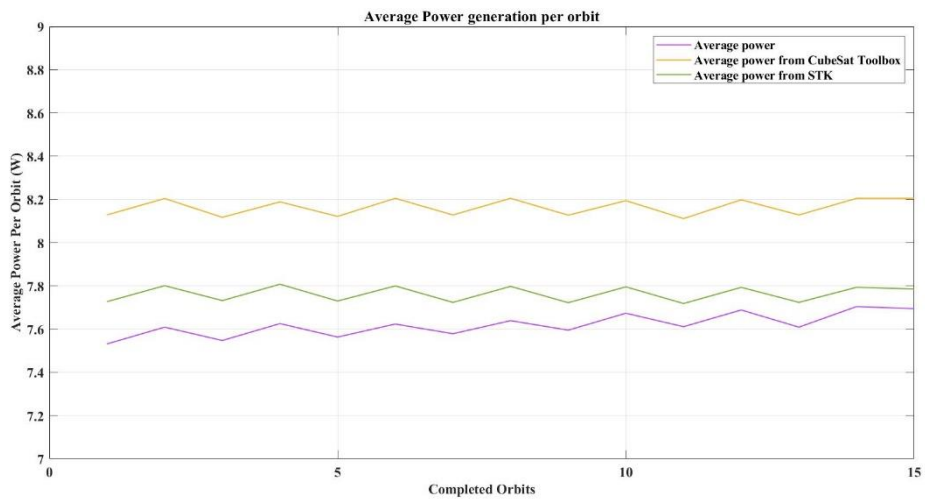


Figure 32: average power generation per orbit comparison in one day for CubeSat Toolbox model



## 5 Power Generation for different 3U CubeSat models

In this chapter, two 3U CubeSats, each with a few different solar panel configurations, are considered. The power generation of different models will be analysed to find which configuration provides the maximum power for the mission. The analysis in this chapter is without considering the self-shadowing effect.

All the models have the same attitude which is nadir pointing in negative Z direction and it is aligned with the velocity in negative X direction. The analysis parameters are:

- Epoch time: 20 March 2021 at 08:00:00 UTCG
- Semi-major axis ( $a$ ) = 6771 km
- Eccentricity ( $e$ ) = 0
- Inclination ( $i$ ) = 51.6
- Time step: 30 second for one day analysis.

### 5.1 Model1

Model1 is a 3U CubeSat in vertical direction with respect to the Z direction. Its designs include five solar panels configurations which are shown in Figure 33. BMP-V includes only body mounted solar panels in all the sides. BM-DP-V-90 is the same as the first, but it includes more four deployable solar panels is 90-degree deployment angle. BM-DP-V-45 is same as BM-DP-V-90, but the deployment angle is 45-degree. For DP-V-90, it does not include any body mounted solar panels except +Z direction and it has four deployable solar panels with 90-degree deployment angle. DP-V-45 has the same design of the previous but with 45-degree deployment angel.

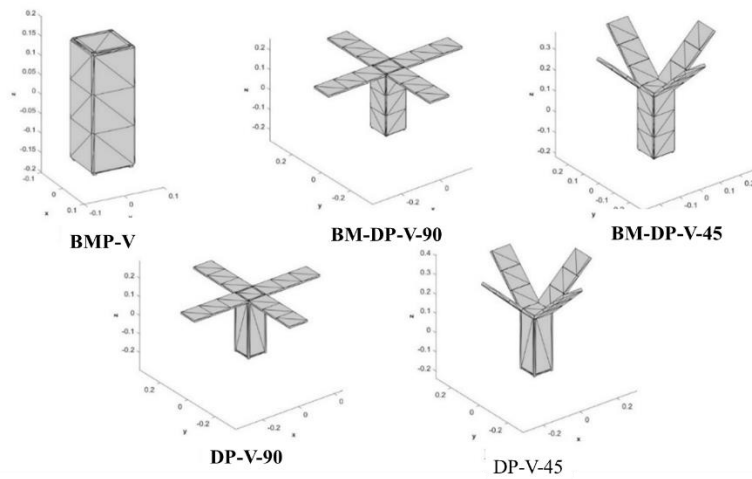


Figure 33: Modell's solar panels configurations

## 5.2 Model2

Model2 is also for a 3U CubeSat, but it is in a horizontal direction with respect to the Z direction. Its designs include three solar panels configurations which are shown in Figure 34. BMP-H includes only body mounted solar panels. BM-DP-H-90 includes four more deployable solar panels on BMP-H. the solar panels deployment angle is 90-degree. BM-DP-H-45 is same as the previous, but the deployment angle is 45-degree.

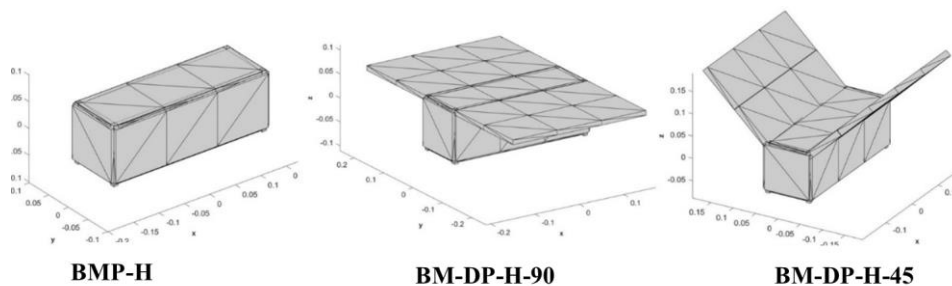


Figure 34: Model2's solar panels configurations

## 5.3 Analysis results

The average power of each configuration results are summarized in Table 2. BMP-V and BMP-H has the same configuration with different orientations where the vertical orientation (BMP-V) produce more power by 14.6%. BM-DP-V-90 generates power higher than BM-DP-V-45 by 23%, which means that 90-degree deployment angle is more efficient for this model. Whereas in Model2, 45-degree deployment angle is more efficient by 30% than 90-degree. By

removing the body-mounted solar panels in DP-V-90, the power generation reduces by 28% and in DP-V-45 decreases by 37%. In addition, BM-DP-V-90 generates more power than BM-DP-H-90 by 38% while BM-DP-H-45 generates more than BM-DP-V-45 by 13%.

Figure 35 shows the power curve of BMP-V without any deployable solar panels. Adding deployable solar panels in positive Z direction with 90-degree increases the peak of the power curve to almost 42 W and makes the curve smoother as in Figure 37. However in BM-DP-V-45 where the deployment angle is 45-degree, the projection of the areas of the solar panels are in X,Y and Z directions which causes the change in the curve in Figure 39. DP-V-90's power curve is shown in Figure 41 which is a very smooth curve because the solar panels are only in one direction which is Z direction. The power curve of DP-V-45 is shown in Figure 43. Figure 37 is almost combination between Figure 35 and Figure 41 whereas Figure 39 is a combination between Figure 35 and Figure 43.

The power curve of BMP-H is shown in Figure 45. Adding deployable solar panels on BMP-H increases the peak of the curve to be almost 28 W for BM-DP-H-90 as shown in Figure 47 and almost 42 W for BM-DP-H-45 as in Figure 49.

The average power per orbit for one day for each model are shown in the below figures.

*Table 2: Summary of Model1 and Model2 results*

<b>Model #</b>	<b>Average power (W)</b>
<b>BMP-V</b>	5.3171
<b>BM-DP-V-90</b>	16.3976
<b>BM-DP-V-45</b>	12.6126
<b>DP-V-90</b>	11.7327
<b>DP-V-45</b>	7.9166
<b>BMP-H</b>	4.5366
<b>BM-DP-H-90</b>	10.0942
<b>BM-DP-H-45</b>	14.514

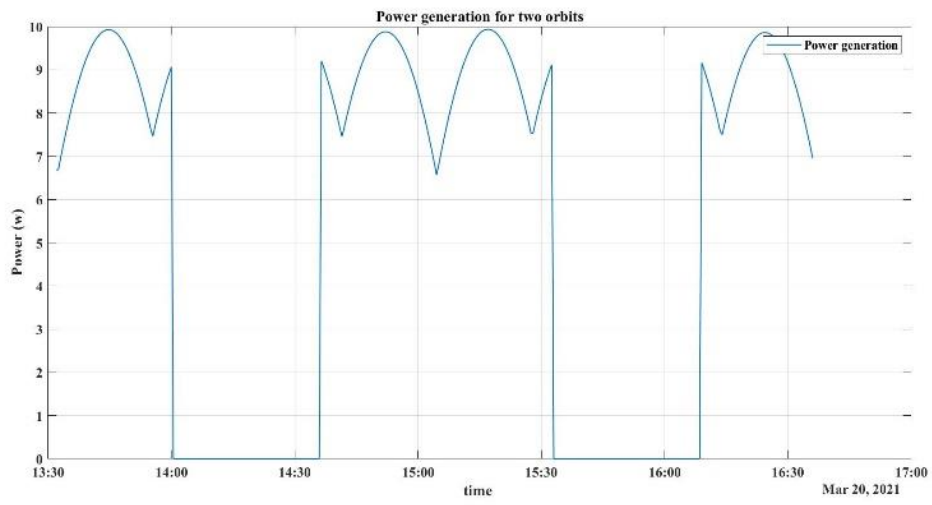


Figure 35: power generation in two orbits for BMP-V

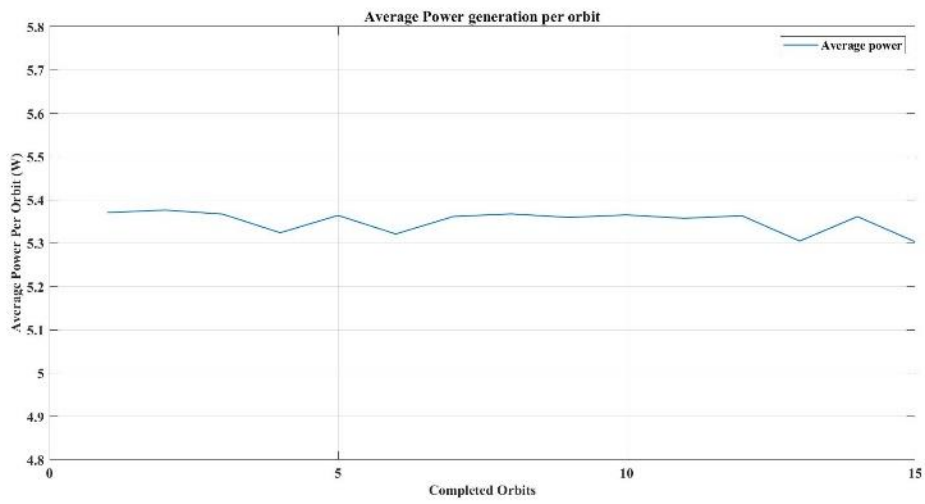


Figure 36: average power generation per orbit in one day for BMP-V

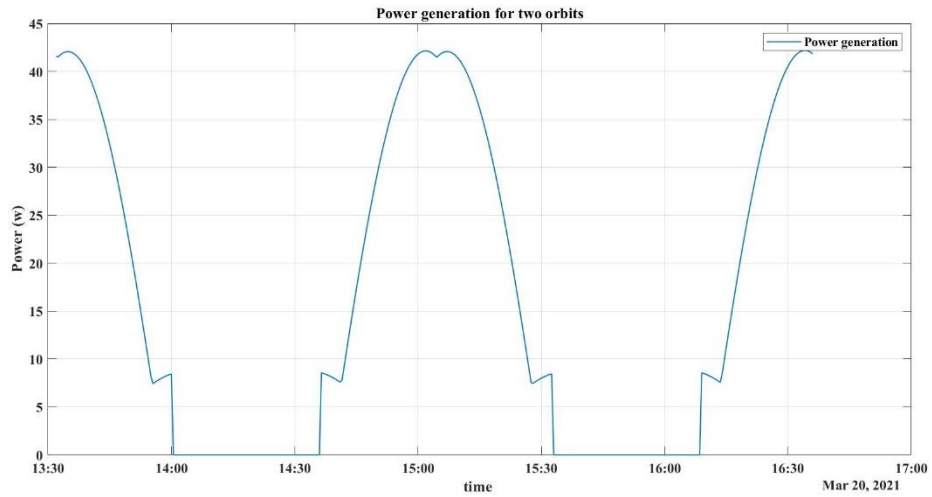


Figure 37: power generation in two orbits for BM-DP-V-90

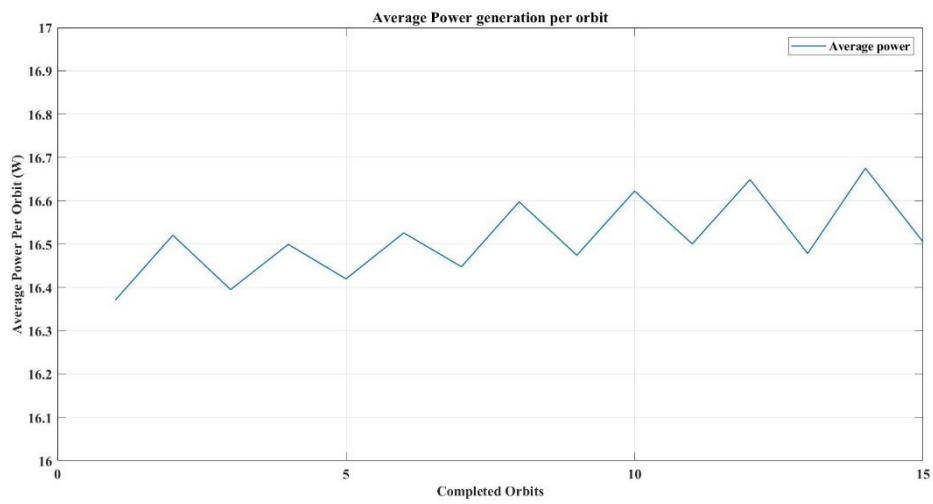


Figure 38: average power generation per orbit in one day for BM-DP-V-90

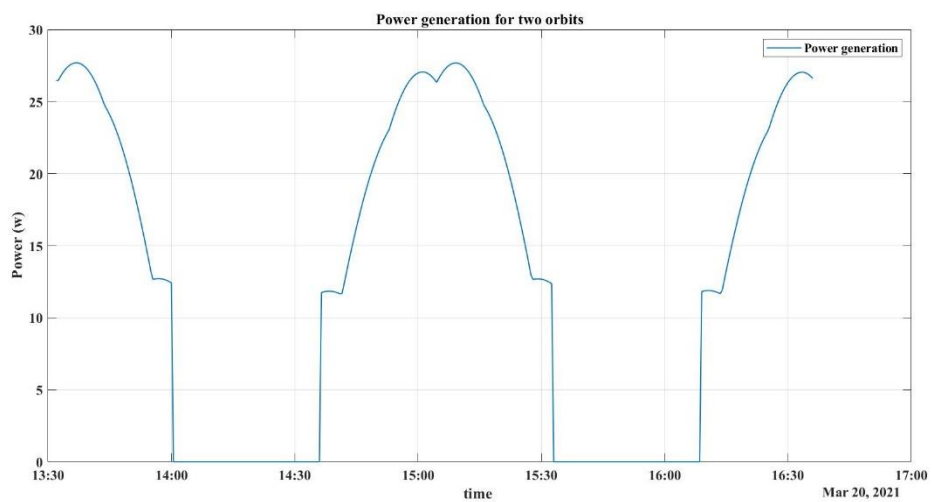


Figure 39: power generation in two orbits for BM-DP-V-45

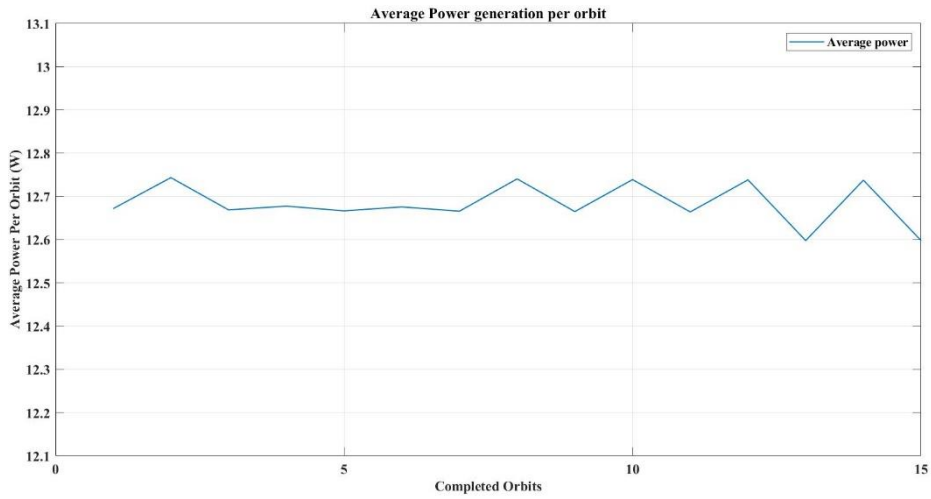


Figure 40: average power generation per orbit in one day for BM-DP-V-45

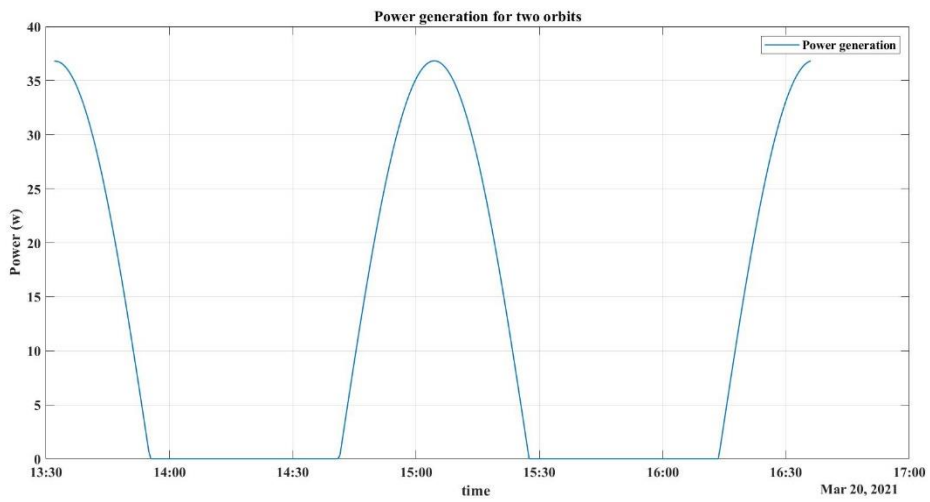


Figure 41: power generation in two orbits for DP-V-90

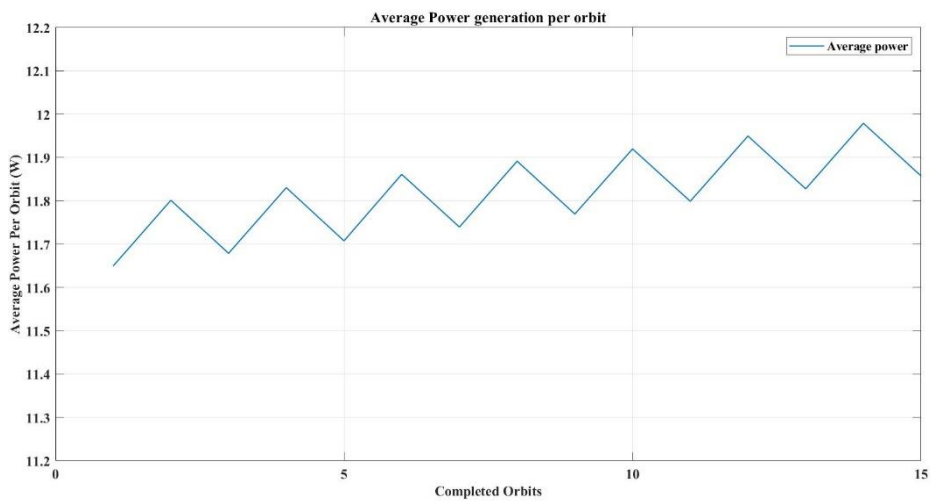


Figure 42: average power generation per orbit in one day for DP-V-90

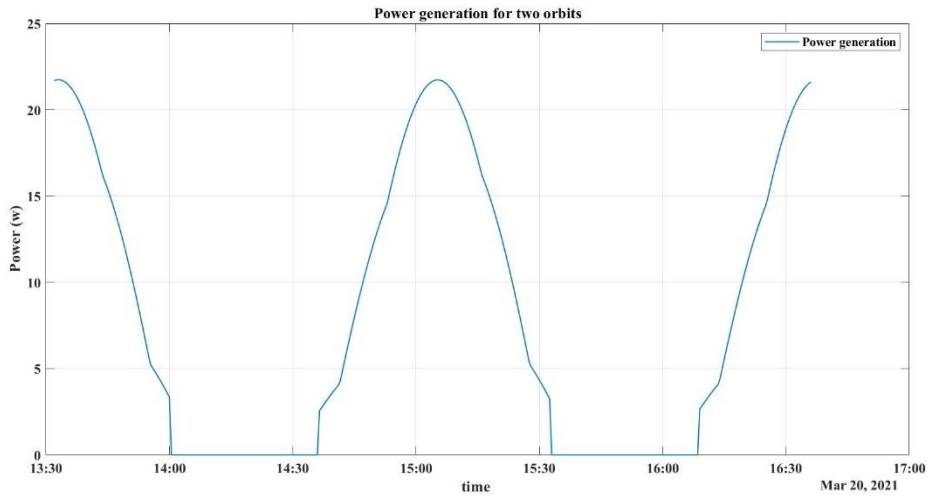


Figure 43: power generation in two orbits for DP-V-45

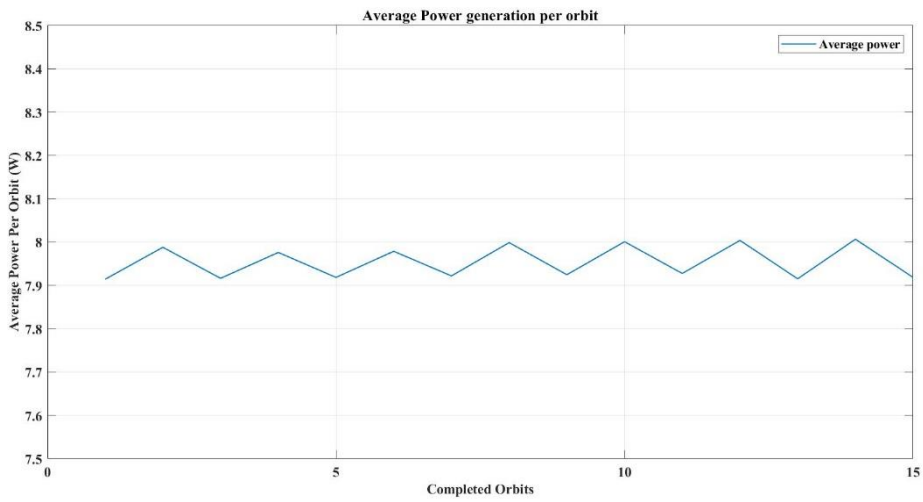


Figure 44: average power generation per orbit in one day for DP-V-45

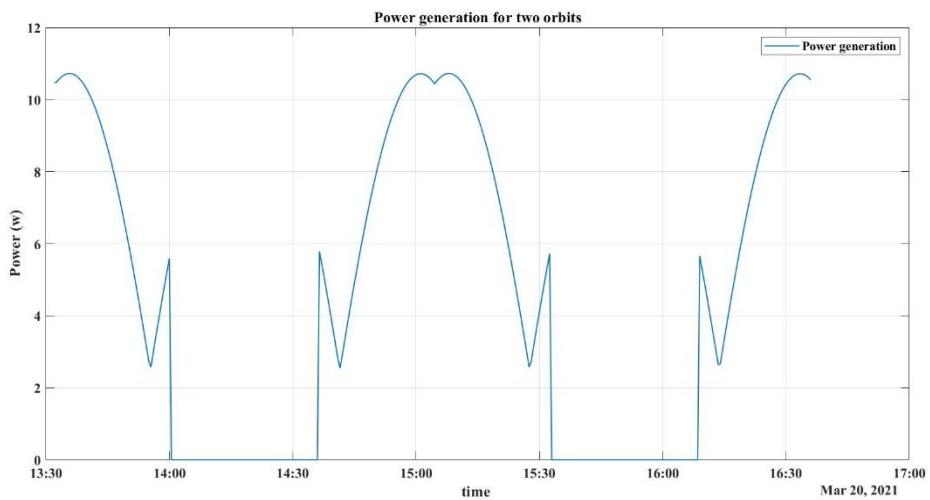


Figure 45: power generation in two orbits for BMP-H

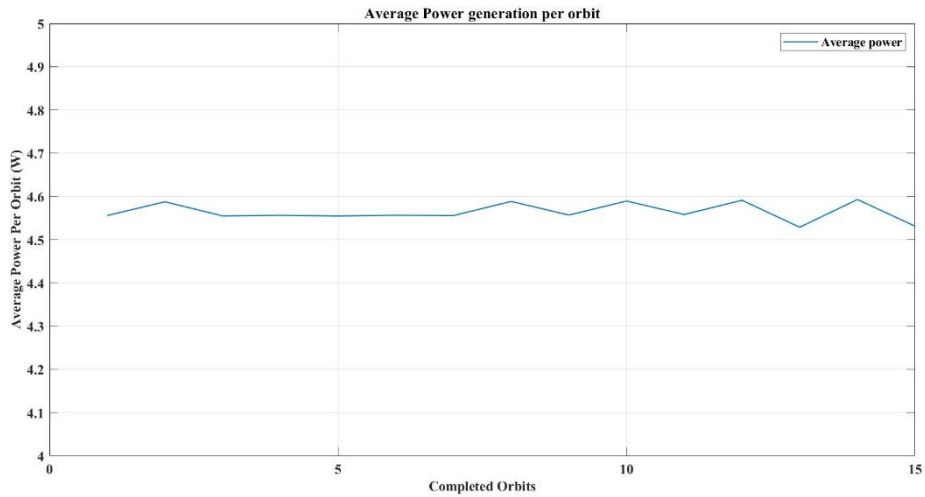


Figure 46: average power generation per orbit in one day for BMP-H

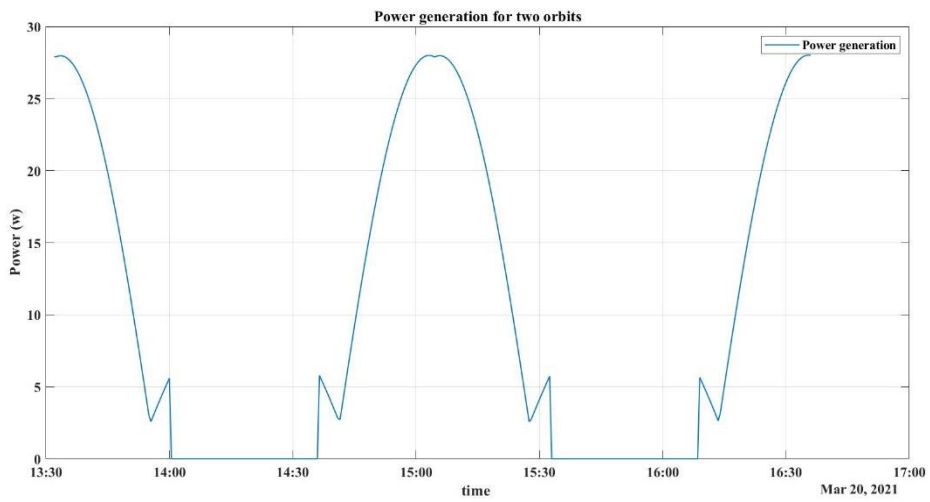


Figure 47: power generation in two orbits for BM-DP-H-90

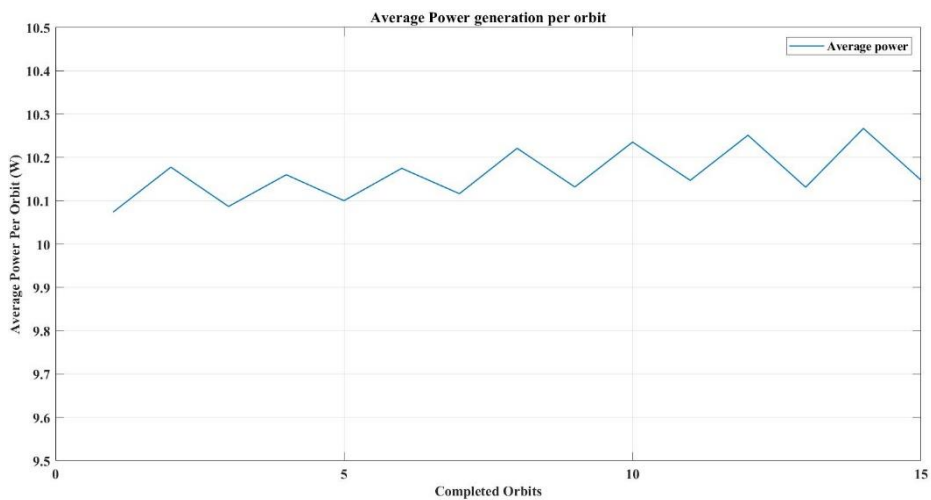


Figure 48: average power generation per orbit in one day for BM-DP-H-90



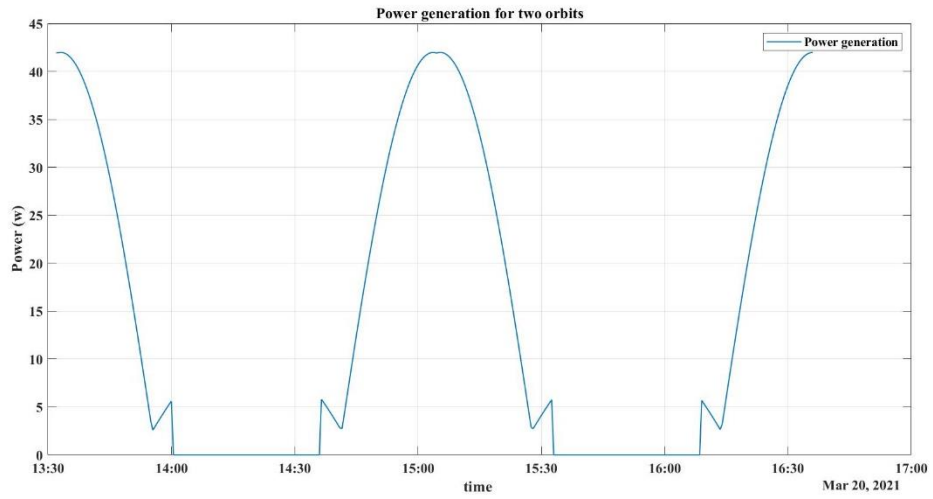


Figure 49: power generation in two orbits for BM-DP-H-45

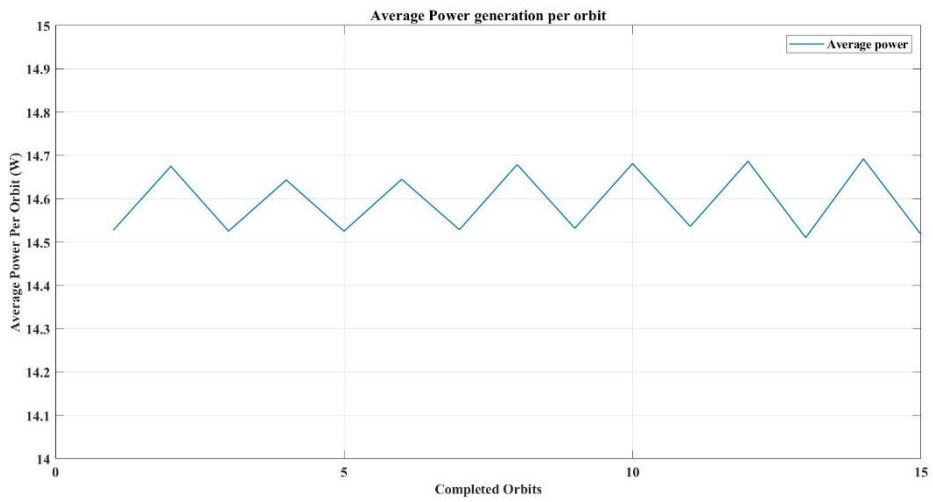


Figure 50: average power generation per orbit in one day for BM-DP-H-45]

## 6 Self-shadowing

One of the major effects on the solar power generation system in the spacecraft is self-shadowing where some parts of the spacecraft shadow the solar panels and reduce the power generation. In this chapter, self-shadowing effect on the body-mounted solar panels caused by the deployable solar panels in the CubeSat will be analyzed.

In general, the power system needs to save enough power during sunlight to survive the periods of eclipse. This can be greatly reduced by the partial shadowing of the solar arrays that take place during sunlight periods when the deployable solar panels produce a shadow on the solar arrays underneath.

Self-shadowing depends on the solar panels' configurations and on the sun position in the sky which depends on the seasons.

One way of simulating the self-shadowing and find the affected area in the CubeSat is by raytracing. Raytracing is a way of checking the sun vector path between the source of light and an object that is lit up by the light. If there is anything in the way it means that there is an intersection which indicates that there is a shadow. In CubeSat, the sun vectors are plotted during the orbit and the intersection between the sun vectors and the deployable solar panels indicates the shaded area of the body-mounted solar panels[24].

The algorithm of raytracing is made using CubeSat toolbox [23]. It has built-in functions that makes it easier to model the sun vectors for a period of time which allow the tracing of the sun vectors through the deployable solar panels and define the shadowed body-mounted solar panel. The algorithm starts by defining the orbital parameters and the date. Then, a 3D model of the CubeSat in the body-frame is modeled. After that, the sun vectors are plotted in the same figure of the CubeSat in the body-frame at each step of the orbit.

### 6.1 Simulation parameters

BM-DP-V-90, BM-DP-V-45, BM-DP-H-90 and BM-DP-H-45 are analyzed for self-shadowing. They were modeled in the four sun seasons which are, winter solstice, vernal equinox, summer solstice and autumnal equinox.

All the models have the same attitude which is nadir pointing in negative Z direction and it is aligned with the velocity in negative X direction. The Epoch times in the simulation parameters

below are chosen based on the beginning of each season. The duration of the simulation was only four hours to simplify the identification process in the figures as longer periods makes a continuous circle which makes the identification of the intersection points difficult.

- Epoch time:
  - Winter: 22 Dec 2021 at 08:00:00 UTCG
  - Vernal: 21 Mar 2021 at 08:00:00 UTCG
  - Summer: 22 Jun 2021 at 08:00:00 UTCG
  - Autumnal: 23 Sep 2021 at 08:00:00 UTCG
- Semi-major axis ( $a$ ) = 6871 km
- Eccentricity ( $e$ ) = 0
- Inclination ( $i$ ) = 51.6
- Time step: 30 second for 4 hours.

## 6.2 Self-shadowing analysis results

An estimation of the self shadowing is done by drawing the instantaneous solar vectors from the CubeSat to the sun where the direction indicates the position of the sun that is changing with respect to the CubeSat as it moves along the orbit as shown in Figure 51. The arrows of the solar vector indicate the position of the sun.

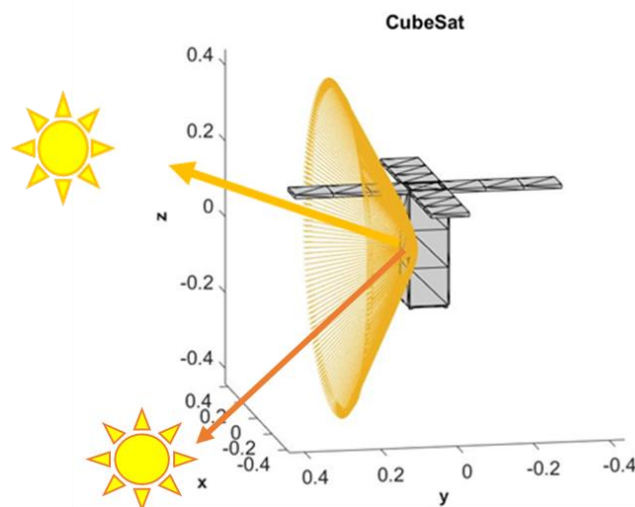


Figure 51: BM-DP-V-90 solar vector plot

Then, the intersection between the vectors and the deployable solar panels is checked. If the intersection presents that means, there is a shadow in the body-mounted solar panels. As shown in where the red circle indicates the shadowed area.

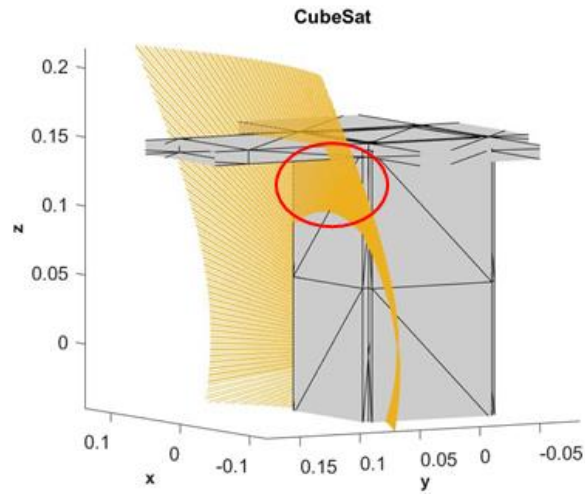


Figure 52: BM-DP-V-90 shadowed area.

The results of the analysis for all the models in different seasons are shown below.

## BM-DP-V-90

### 1. Winter solstice

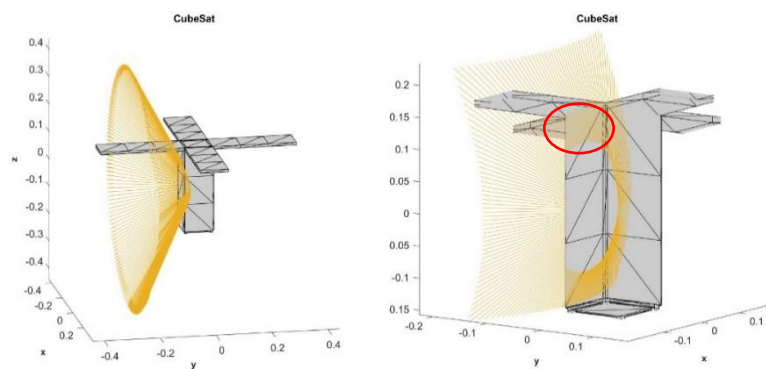


Figure 53: BM-DP-V-90 raytracing in winter solstice

## 2. Vernal equinox

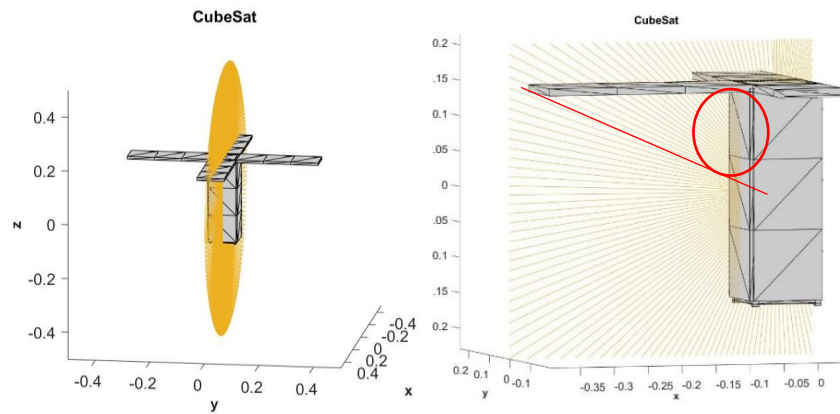


Figure 54: BM-DP-V-90 raytracing in vernal equinox

## 3. Summer solstice

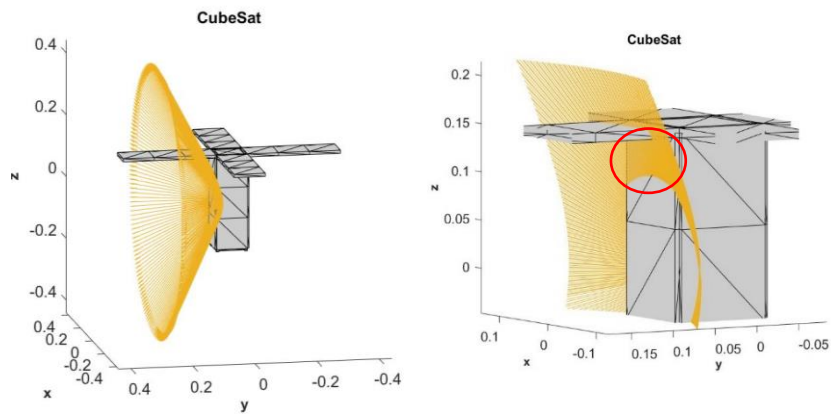


Figure 55: BM-DP-V-90 raytracing in summer solstice

## 4. Autumnal equinox

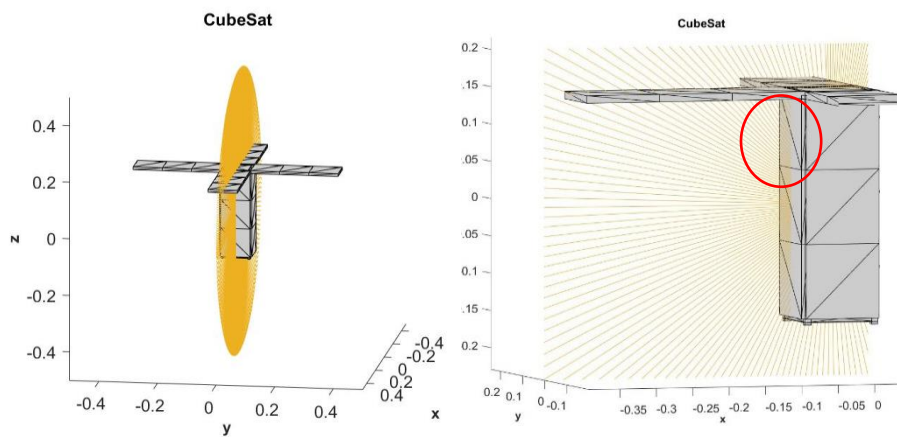


Figure 56: BM-DP-V-90 raytracing in autumnal equinox

For BM-DP-V-90, almost half solar panel (one solar cell) will be affected during winter and summer solstices as shown in Figure 53 and Figure 55. It is the first one in negative Y face of the CubeSat in the summer solstice whereas it is in positive Y face in the winter solstice. However, during vernal and autumnal equinoxes, almost one and half solar panel (3 solar cells) in both positive X and negative X faces of the CubeSat will be shadowed as Figure 54 and Figure 56 illustrate.

## BM-DP-V-45

### 1. Winter solstice

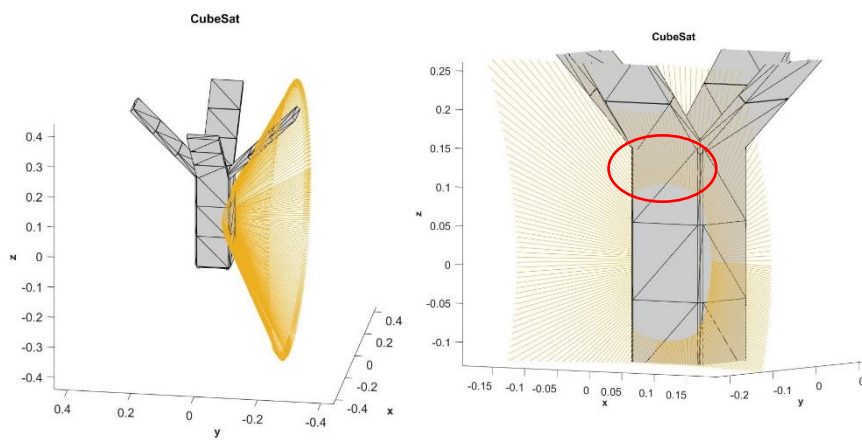


Figure 57: BM-DP-V-45 raytracing in winter solstice

### 2. Vernal equinox

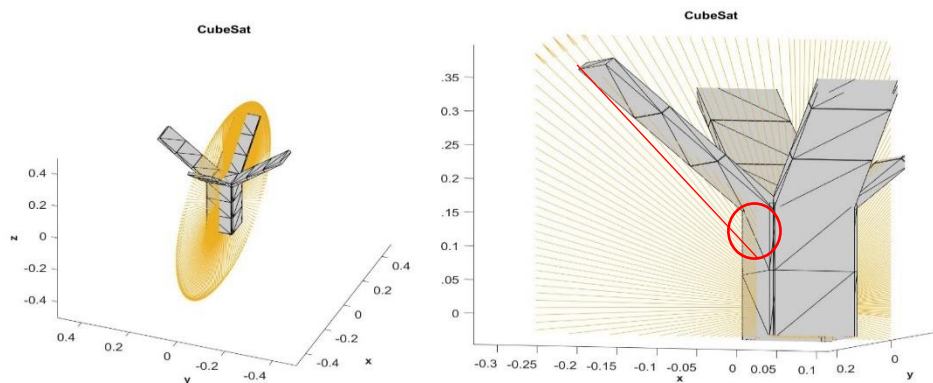


Figure 58: BM-DP-V-45 raytracing in vernal equinox

### 3. Summer solstice

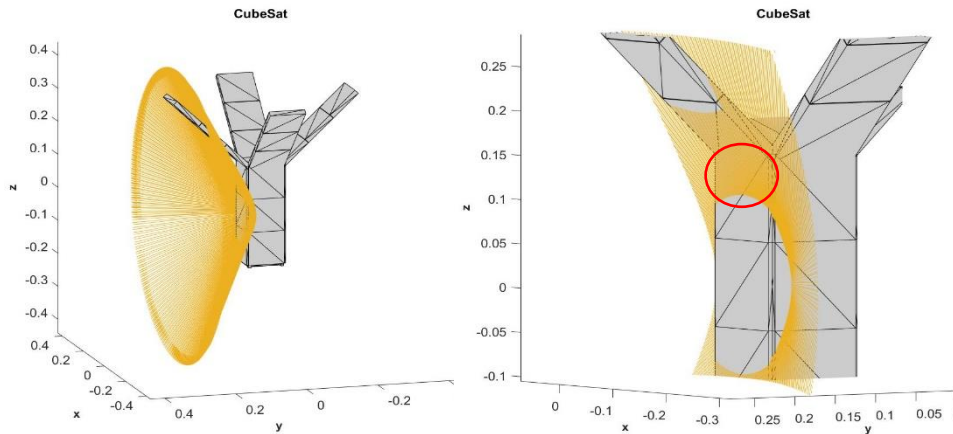


Figure 59: BM-DP-V-45 raytracing in summer solstice

### 4. Autumnal equinox

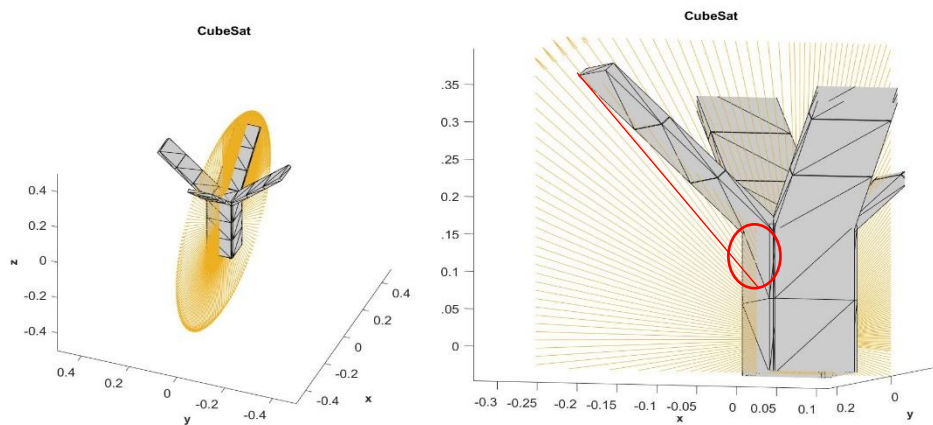


Figure 60: BM-DP-V-45 raytracing in autumnal equinox

Self-shadowing effect in BM-DP-V-45 is almost the same as BM-DP-V-90 although it is less affected in vernal and autumnal equinoxes where only one solar panel is affected in both positive X and negative X sides of the CubeSat instead of one and half solar panels in BM-DP-V-90.



# BM-DP-H-90

## 1. Winter solstice

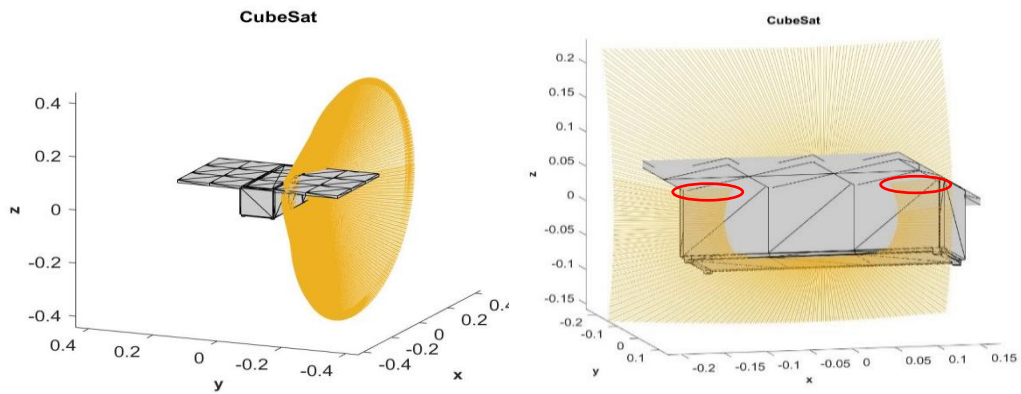


Figure 61: BM-DP-H-90 raytracing in winter solstice

## 2. Vernal equinox

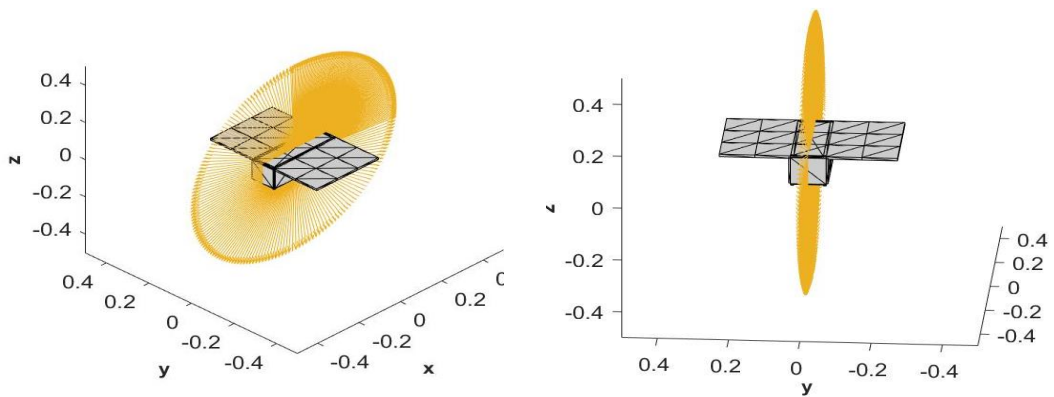


Figure 62: BM-DP-H-90 raytracing in vernal equinox

## 3. Summer solstice

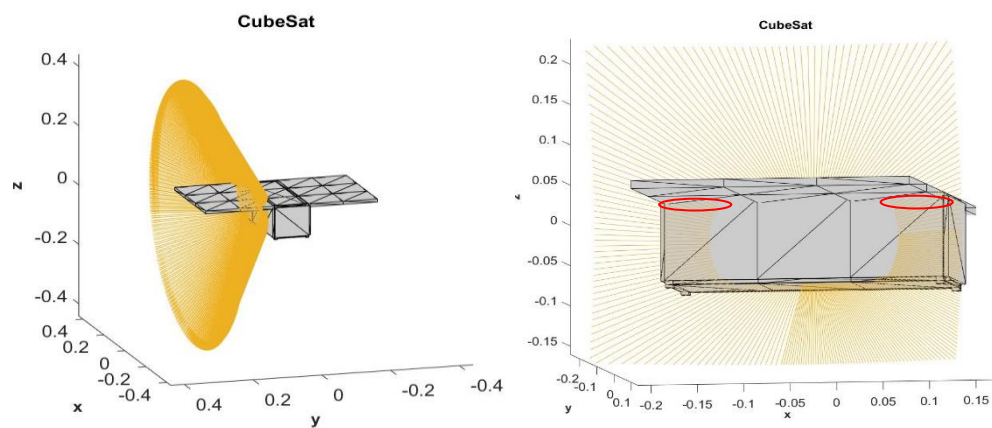


Figure 63: BM-DP-H-90 raytracing in summer solstice



#### 4. Autumnal equinox

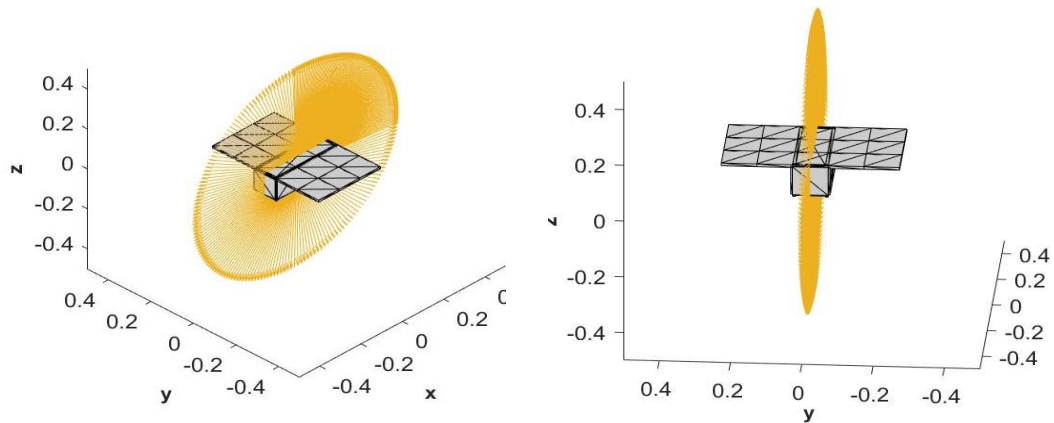


Figure 64: BM-DP-H-90 raytracing in autumnal equinox

BM-DP-H-90 exposes to a minor self-shadowing effect during winter and summer solstices. As Figure 61 shows, very small area of two solar cells in negative Y face of the CubeSat will be affected during winter solstice. The same effect occurs in summer solstice but it occurs in positive Y face as shown in Figure 63. There is no self-shadowing effect in vernal and autumnal equinoxes as Figure 62 and Figure 64 illustrate.

### BM-DP-H-45

#### 1. Winter solstice

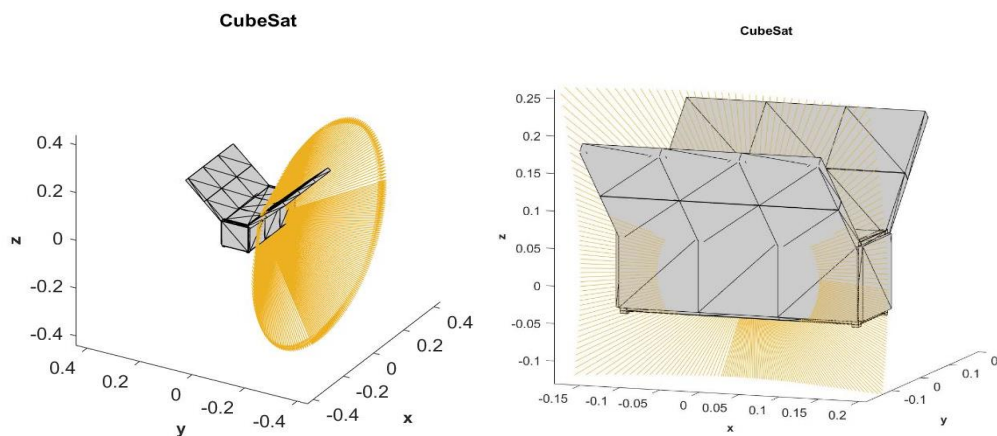


Figure 65: BM-DP-H-45 raytracing in winter solstice

## 2. Vernal equinox

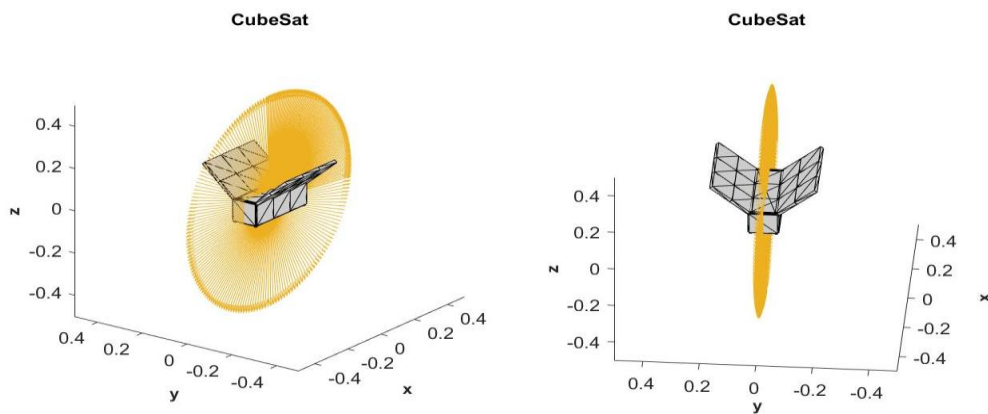


Figure 66: BM-DP-H-45 raytracing in vernal equinox

## 3. Summer solstice

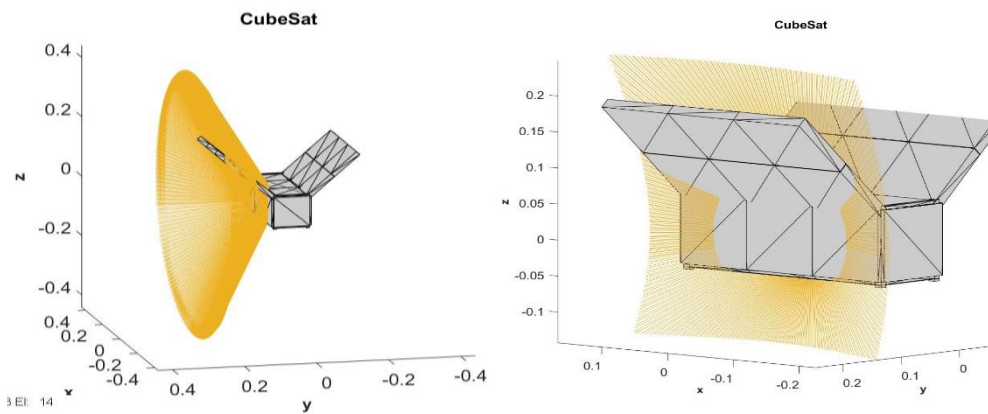


Figure 67: BM-DP-H-45 raytracing in summer solstice

## 4. Autumnal equinox

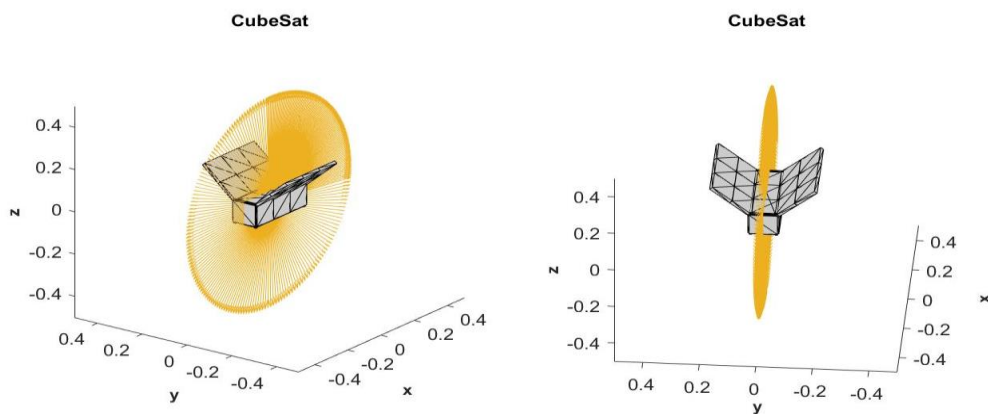


Figure 68: BM-DP-H-45 raytracing in autumnal equinox

There is no self-shadowing effect in BM-DP-H-45 as Figure 65 to Figure 68 show.

### 6.3 Self-shadowing effect on power generation

The power generation could be affected by the shaded solar cells as they do not generate any power. The power generation will be computed for the affected models with considering removing the shaded cells. Applying the same analysis parameters:

- Epoch time: 21 March 2021 at 08:00:00 UTCG
- Semi-major axis (a) = 6771 km
- Eccentricity (e) = 0
- Inclination (i) = 51.6
- Time step: 30 second for one day analysis.

The shading effect will be considered in vernal equinox. For BM-DP-V-90, three solar cells will be removed from both positive and negative X faces. whereas for BM-DP-V-45, it will be only two solar cells. However, BM-DP-H-90 and BM-DP-H-45 do not experience any self-shadowing effect during vernal equinox even in winter and summer solstices BM-DP-H-90 experiences a minor self shadowing effect.

The results are summarized in Table 3. The power generation throughout the orbit for BM-DP-V-90 without considering and with considering the self-shadowing is shown in Figure 69 and Figure 70. As illustrated in Figure 70, the reduction in power is mostly occur in the side peaks of the curve because the effected side is the negative Y. The average power per orbit for BM-DP-V-90 is shown in Figure 71. Considering the self-shadowing effect reduces the power by 9% which could be critical in some missions.

However, the power generation curves with considering self-shadowing effect for BM-DP-V-45 are shown in Figure 72 and Figure 73. The power reduction in Modle1\_C power curve is illustrated in Figure 73 . The average power per orbit is shown in Figure 74. The power in BM-DP-V-45 is reduced by almost 8%.

Table 3: Results of power generation considering self-shadowing

Model	Power Generation (W)	
	Without considering self-shadowing	Considering self-shadowing
<b>BM-DP-V-90</b>	16.3976	14.834
<b>BM-DP-V-45</b>	12.6162	11.5737

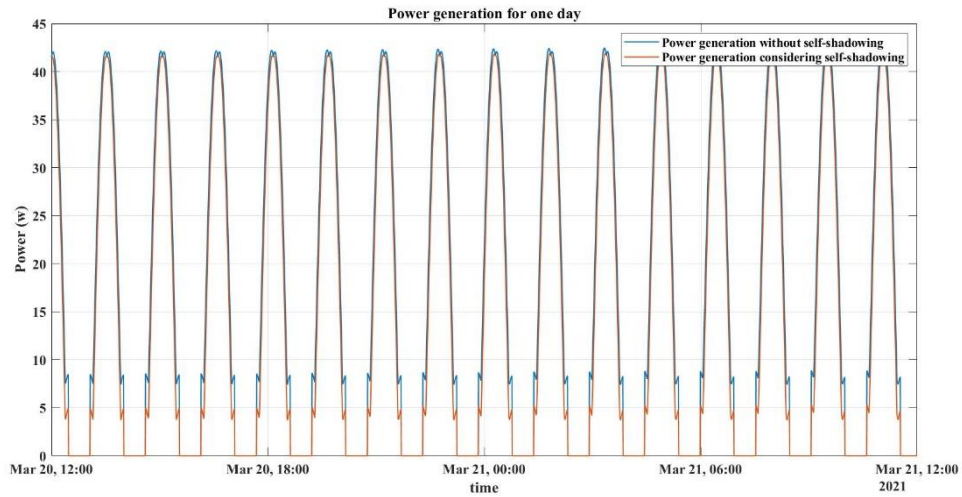


Figure 69: BM-DP-V-90 power generation in one day with considering the self-shadowing



Figure 70: BM-DP-V-90 power generation in two orbits with considering the self-shadowing

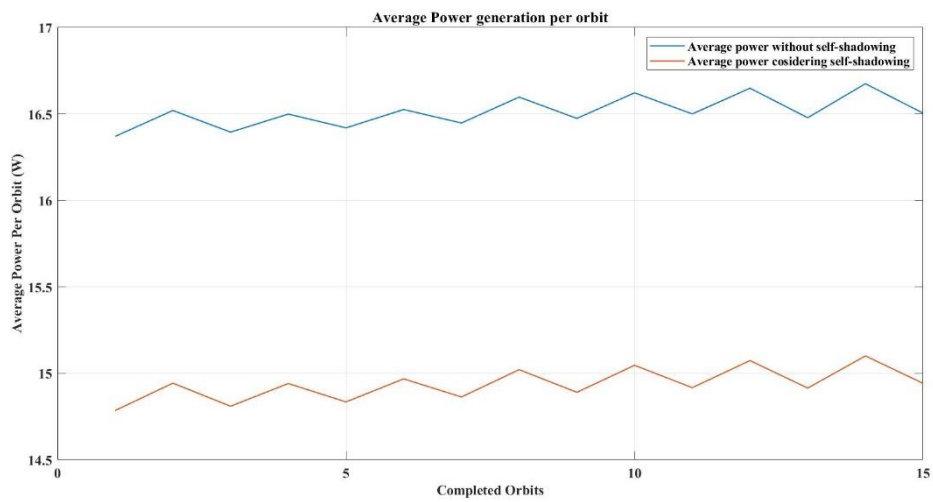


Figure 71: Average power generation per orbit in one day for BM-DP-V-90 with considering self-shadowing

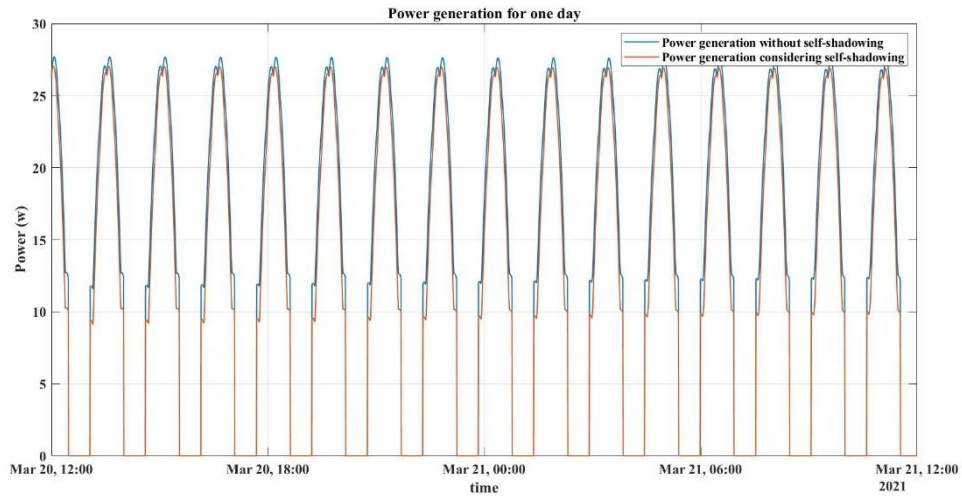


Figure 72: BM-DP-V-45 power generation in one day with considering the self-shadowing

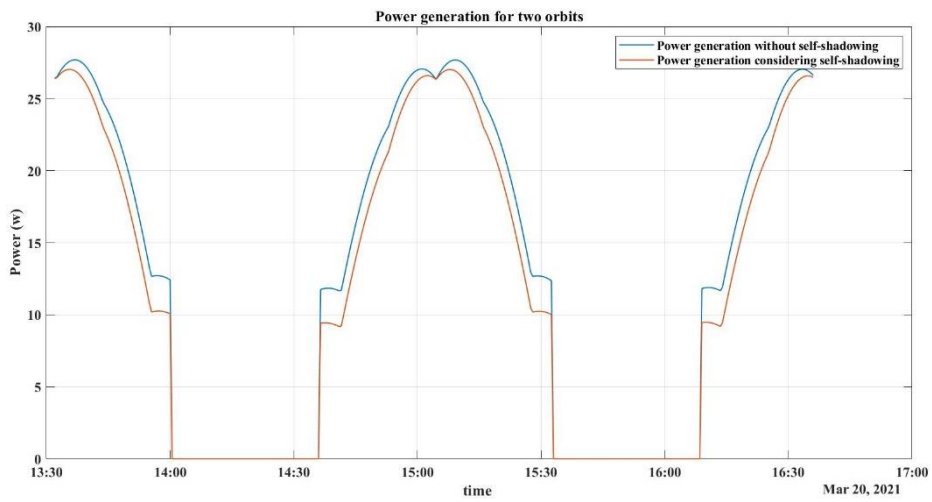


Figure 73: BM-DP-V-45 power generation in two orbits with considering the self-shadowing

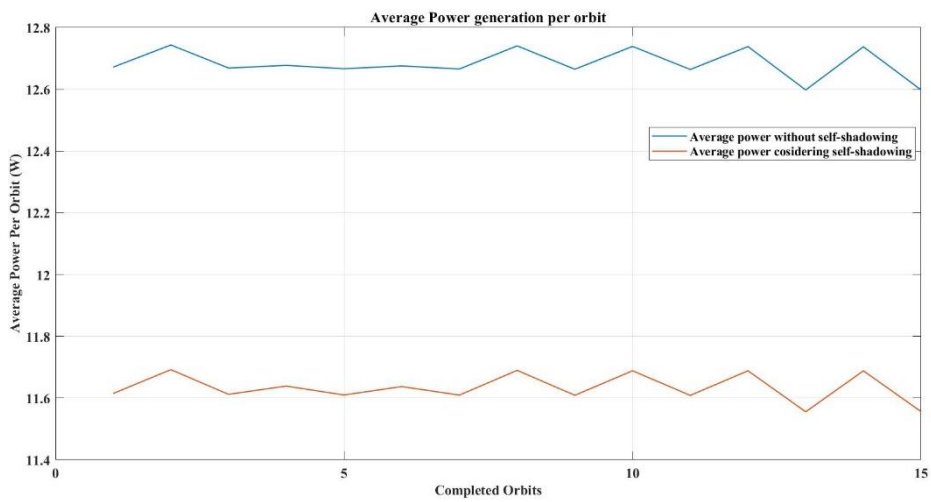


Figure 74: Average power generation per orbit in one day for BM-DP-V-45 with considering self-shadowing

## 7 Conclusion and recommendations

This research describes the MATLAB algorithm for estimating the power generation throughout the orbit of a CubeSat with using the General Mission Tool (GMAT) to simulate the orbit and the CubeSat attitude. The MATLAB code then verified by comparing its output to the results obtained using the Satellite Tool Kit (STK) and the results from the CubeSat Toolbox code. The power generation throughout the orbit has been obtained for different eight solar panels configurations for a 3U CubeSat with nadir pointing toward the earth in Low Earth orbit. The analysis results show that adding deployable solar panels increases the power dramatically as in BM-DP-V-90 and BM-DP-V-45. In addition, deploying the body-mounted solar panels will increase the power generation as in DP-V-90 and DP-V-45.

An estimation of self-shadowing effect by the deployable solar panels on the body-mounted solar panels is carried out in this research. The self-shadowing was estimated using raytracing method and it was done in different sun seasons where the sun's position changes with respect to Earth. The self-shadowing effect of the power generation is studied for two models in vernal equinox and it shows that the power generation could be reduced by almost 10% which could be very critical for some CubeSats missions.

The analysis can be carried out for longer duration of time which could be as long of the mission plan that goes up to six months. Also, self-shadowing algorithm could be more enhanced to simulate different seasons together.

## References

- [1] California State Polytechnic University, *CubeSat Design Specification*, Rev 13. USA, CA: California State Polytechnic University, 2014.
- [2] J. Chin *et al.*, “CubeSat 101: Basic Concepts and Processes for First-Time CubeSat Developers,” no. October, p. 96, 2017.
- [3] “The CubeSat phenomenon.” [Online]. Available: <https://cceres.psl.eu/spip.php?rubrique21&lang=en>. [Accessed: 19-Apr-2019].
- [4] A. Poghosyan and A. Golkar, “CubeSat evolution: Analyzing CubeSat capabilities for conducting science missions,” *Prog. Aerosp. Sci.*, vol. 88, pp. 59–83, Jan. 2017.
- [5] S. S. Technology, “State of the Art Small Spacecraft Technology,” 2018.
- [6] E. Agasid *et al.*, “Small Spacecraft Technology State of the Art,” *NASA Ames Res. Center, Mission Des. Div.*, no. September, 2015.
- [7] H. Park and H. Cha, “Electrical Design of a Solar Array for LEO Satellites,” *J. Aeronaut. Sp. Sci.*, vol. 17, no. 3, pp. 401–408, 2016.
- [8] A. Solís-Santomé *et al.*, “Conceptual design and finite element method validation of a new type of self-locking hinge for deployable CubeSat solar panels,” *Ing. Mecánica en España-Mechanical Eng. Spain-Research Artic. Adv. Mech. Eng.*, vol. 11, no. 1, pp. 1–13, 2019.
- [9] F. Santoni, F. Piergentili, S. Donati, M. Perelli, A. Negri, and M. Marino, “An innovative deployable solar panel system for Cubesats,” *Acta Astronaut.*, vol. 95, pp. 210–217, 2014.
- [10] R. Surampudi *et al.*, “Solar power technologies for future planetary science missions,” *NASA/Jet Propuls. Lab.*, no. December, 2017.
- [11] C. Clark, “Huge Power Demand...Itsy-Bitsy Satellite: Solving the CubeSat Power Paradox,” *24th Annu. AIAA/USU Conf. Small Satell.*, no. August, pp. 1–8, 2010.
- [12] “Orbital elements.” [Online]. Available: [https://en.wikipedia.org/wiki/Orbital\\_elements](https://en.wikipedia.org/wiki/Orbital_elements). [Accessed: 05-Apr-2019].

- [13] T. Logsdon, *Orbital Mechanics: Theory and Applications*. 1998.
- [14] “Orbital and Technical Parameters | European GNSS Service Centre.” [Online]. Available: <https://www.gsc-europa.eu/system-service-status/orbital-and-technical-parameters>. [Accessed: 02-Nov-2019].
- [15] D. Young, J. W. Cutler, J. Mancewicz, and A. J. Ridley, “Maximizing photovoltaic power generation of a space-dart configured satellite,” *Acta Astronaut.*, vol. 111, pp. 283–299, 2015.
- [16] S. Sanchez-sanjuan, J. Gonzalez-llorente, and R. Hurtado-velasco, “Comparison of the Incident Solar Energy and Battery Storage in a 3U CubeSat Satellite for Different Orientation Scenarios,” vol. 8, no. 14, pp. 91–102, 2016.
- [17] A. Abdulkarim, “Maximizing Photovoltaic Power Generation for 3U CubeSat by Optimal Design Maximizing Photovoltaic Power Generation for 3U CubeSat by Optimal Design by,” Khalifa University, 2018.
- [18] P. Senatore, A. Klesh, T. H. Zurbuchen, D. McKague, and J. Cutler, “Concept, Design, and Prototyping of XSAS: A High Power Extendable Solar Array for CubeSat Applications,” *40th Aerosp. Mech. Symp.*, pp. 431–444, 2010.
- [19] B. Kading, J. Straub, and D. J. Whalen, “A Novel Deployable Array Architecture for Micro to Full Sized Satellites,” no. August, pp. 1–11, 2014.
- [20] “A CubeSat Deployable Solar Panel System,” vol. 9865, pp. 1–8, 2016.
- [21] GOMSpace, “NanoPower Datasheet,” pp. 1–19, 2018.
- [22] “2RU Generic CubeSat | 3D Resources.” [Online]. Available: <https://nasa3d.arc.nasa.gov/detail/cubesat-2RU>. [Accessed: 29-May-2020].
- [23] “CubeSat Toolbox | Princeton Satellite Systems.” [Online]. Available: <http://www.psatellite.com/products/sct/cubesat-toolbox/>. [Accessed: 14-Jun-2020].
- [24] S. Callbo, S. För, and E.-O. C. H. Systemteknik, “Solar Cell Current Simulator for a 3U Cube Satellite Master thesis within the MIST project,” 2016.



## Appendix

- **Self-Shadowing code:**

**This code is adjusted by me from the power generation demo provided by CubeSat toolbox to plot the sun vector during the orbit for a duration of 4 hours.**

```
%% Plot Sun vectors on the CubeSat
%% Constants
solarFlux = 1367; % W
radiusEarth = 6371; % km
altitude = 500; % km
inc = 51.6*pi/180; % deg
sma = radiusEarth + altitude; %km

%% date in Julian Centuries for the sun model
jd0 = Date2JD([2021 06 22 8 0 0]); %input the date and time
t = linspace(0,4*3600,480); % define the duration
julianDate = jd0 + t/86400;
T = julianDate.';
T= datetime(T,'convertfrom','juliandate','Format','dd/MM/yyyy
HH:mm:ss' );

%% Compute trajectory from orbital elements
[rs,vs,t] = RVFromKepler( [sma inc 0 0 0 0], t );
m = length(t);

%% CubeSat model including the deployed solar panels
d = CubeSatModel( 'struct' );
d.massComponents = 3;
d.solarPanel.dim = [100 100 10]; % [side attached to cubesat,
side perpendicular, thickness]
d.solarPanel.nPanels = 1; % Number of panels per wing
d.solarPanel.rPanel = [-150 -50 50 -150 -50 50 -150 150 -100 0
100 -100 0 100 -150 -50 50 -150 -50 50 -150 -50 50 -150 -50 50 ;
0 0 0 0 0 0 -50 -50 -50 -50 -50 50 50
50 -80 -80 -80 80 80 80 -150 -150 -150 150 150 150;
50 50 50 -50 -50 -50 0 0 -50 -50 -50
-50 -50 -50 80 80 80 80 80 80 150 150 150 150 150 150 ]; % Location
of inner edge of panel
d.solarPanel.sPanel = [ 1 1 1 1 1 1 0 0 0 0 0 0 0 0 0 1 1 1 1 1
1 1 1 1 1 1 1; 0 0 0 0 0 0 1 1 0 0 0 0 0 0 0 0 0 0 0 0 0 0 0 0
0; 0 0 0 0 0 0 0 0 1 1 1 1 1 1 0 0 0 0 0 0 0 0 0 0 0 0];
d.solarPanel.cellNormal = [ 0 0 0 0 0 0 -1 1 0 0 0 0 0 0 0 0 0 0 0 0 0
0 0 0 0 0 0 0; 0 0 0 0 0 0 0 0 -1 -1 -1 1 1 1 1 1 1 -1 -1 -1 1 1
1 -1 -1 -1; 1 1 1 -1 -1 -1 0 0 0 0 0 0 0 0 0 1 1 1 1 1 1 1 1 1 1
1]; % Cell normal

[v, f, data] = CubeSatModel( [3 1 1], d );
hF = DrawCubeSat( v, f, data );
```

```

%% Initialize the array
dT          = t(2) - t(1);
tE          = 0;
p           = zeros(1,m);
nEcl       = zeros(1,m);
uSunBody   = zeros(3,m);
uNadir     = zeros(3,m);

%% Track LVLH coordinates;
% z is in the -r direction
% y is in the -rxv direction
% x completes the set; along v in a circular orbit
% q transforms from ECI to LVLH coordinates
qs         = QVLH(rs,vs);
qPoint = Eul2Q( [0;pi;0] ); % Rotate +x to nadir (90 deg rotation
around body Y)

%% Compute the power in a loop
for k = 1:m
    [uSun, rSun] = SunV1( julianDate(k) ); % find the sun vector in
the earth-centered inertial frame.
    qECIToBody   = QMult( qs(:,k), qPoint ); % find the cubesat
bodyframe with Nadir pointing
    uSunBody(:,k) = QForm(qECIToBody,uSun); % the vector to the sun in
the body frame

    figure(hF)
    hA = gca;

    quiver3(0,0,0,uSunBody(1,k),uSunBody(2,k),uSunBody(3,k),0.5,'color',
[0.93 0.69 0.13]);
    aa = axis;
    limit = max(abs(aa));
    axis(limit*[-1 1 -1 1 -1 1]);
end

```